AN INVESTIGATION OF THE VERTICAL VARIATION OF LIGHT SCATTERING IN MONTEREY BAY

CHARLES H. BASSETT
and
HARRY C. FURMINGER

AN INVESTIGATION OF THE VERTICAL VARIATION OF LIGHT SCATTERING IN MONTEREY BAY, CALIFORNIA

* * * * *

Charles H. Bassett, Jr.

and

Harry C. Furminger

AN INVESTIGATION OF THE VERTICAL VARIATION OF LIGHT SCATTERING IN MONTEREY BAY, CALIFORNIA

by

Charles H. Bassett, Jr.
Lieutenant, United States Navy

and

Harry C. Furminger
Lieutenant, United States Navy

Submitted in partial fulfillment of
the requirements for the degree of

MASTER OF SCIENCE

United States Naval Postgraduate School
Monterey, California

1965

AN INVESTIGATION OF THE VERTICAL VARIATION OF LIGHT SCATTERING IN MONTEREY BAY, CALIFORNIA

by

Charles H. Bassett, Jr.

and

Harry C. Furminger

This work is accepted as fulfilling
the thesis requirements for the degree of
MASTER OF SCIENCE

from the
United States Naval Postgraduate School

ABSTRACT

An investigation of the vertical variations of the scattering coefficients for visible light at a selected location in Monterey Bay, California, was conducted during December, 1964, January and February, 1965. Forty-six water samples were collected at various depths on five separate sampling days. Where possible, concurrent light attenuation (horizontal) and solar light extinction measurements were made in situ. The water samples collected were analyzed for density and inorganic phosphates.

From the scattering coefficients computed, and hand-fitting of scattering function curves with theoretical curves, the particle size and particle concentration was estimated for each sample.

The relationships between the sea water density, phosphate content, and the empirically derived scattering coefficient, particle size, and particle concentration were examined. The only significant correlation found is that between particle size and particle concentration. A particle concentration maximum was observed above and adjacent to the pycnocline where one existed.

TABLE OF CONTENTS

TABLE OF CONTENTS

LIST OF TABLES

LIST OF ILLUSTRATIONS

1. Introduction

1.1 Purpose

In recent years, much research effort has been expended in the field of underwater optics, due primarily to the fact that many of the parameters in physical, biological, and chemical oceanography depend upon the physics associated with the transmission of light through sea water. Scientists are now investigating the areal distribution of the horizontal light attenuation as it varies with depth; (Hughes, R., at the Naval Ordnance Test Station, China Lake, California, personal communication); also under investigation is the areal variation of light scattering [35]. The next logical step is a more detailed study of the vertical variation of light scattering; and its causes, effects, and methods of investigation. In this paper the approach to light scattering is through a study of the variation of light scatterers. From such a study, parameters involved in several oceanographic disciplines may be forecast, resulting in the application of research in underwater light transmission to areas such as:

1. development of an underwater coherent light source for use in detection, ranging and communication;
2. the use of attenuation coefficients or scatter coefficients as a means of typing water;
3. the general improvement of underwater photography and television techniques;
4. the study of the penetration of sea water by solar radiation and the resulting effect on productivity;

5. the study of solar radiation penetration and its effect on sea surface temperature and ocean thermal structure.

This investigation emphasizes the utility of scattering analysis as an integral part of descriptive oceanography. This study began in December, 1963, with field sampling beginning a year later. During this time, the authors investigated the oceanographic climatology of the Monterey Bay Area to determine the best sampling area. The sampling area finally chosen was selected considering proximity to shore, water depth, and availability of past oceanographic data [8, 32].

1.2 Theory

Before discussing the variation of scatterers, the applicable definitions and physical relationships for light transmission through water should be reviewed.

1.2.1 Light Attenuation

The attenuation of light is the diminution of intensity of a light beam during its passage through a medium such as sea water, and it results from a number of processes. As shown by Tyler, et. al., this attenuation is mainly attributable to the scattering and absorbing properties of the medium [23].

The function expressing the attenuation of light transmission through a medium is

$$N_r = N_o e^{-\alpha \ell}, \tag{1}$$

an expression of Beer's Law as interpreted by Tyler [11]. N_o and N_r are the source and receiver intensity, respectively, as measured by an "Alpha" (attenuation) meter. The range ℓ is the measured distance between the source and the receiver. A plot of various ranges compared with $\ell n(N_r/N_o)$ should give a straight line when plotted against the total attenuation coefficient of the light beam, α.

The attenuation coefficient is primarily the sum of the total scattering coefficient, S, and the absorption coefficient, a, or

$$\alpha = a + S \tag{2}.$$

These coefficients have the units of length^{-1} .

In a medium such as sea water, the presence of contaminants and solutes alters the scattering and the absorption. In fact, any diatomic molecule of the medium or solute will be a source of possible attenuation [10].

1.2.2 Light Absorption

Scattering is a process which results in the redirection of light energy. Light absorption, in contrast, is a process which is an energy transformation. The absorbing substance diminishes the incident light energy by changing it into other forms of energy, such as heat energy and molecular (rotational) energy [10].

The measurement of absorption coefficients may be complicated and sometimes measurement is performed by indirect means [22]. To measure absorption in a medium such as sea water, it is desirable to use a collimated light source to reduce scattering to a minimum; the optimum source is a highly collimated laser beam. Because of the monochromatic properties of sea water, the usual approach is to use a narrow band sharp cut-off filter with a mercury arc lamp as a light source for optical studies. This source-filter combination will limit the band width of study to the area in the light spectrum where absorption is minimum [11, 18, 30]. The incident light wavelength used in this study was in the band of minimum absorption so as to reduce the variation of absorption, and to concentrate attention on the variation of the scattering properties of sea water.

A direct measurement of absorption is a problem because it involves energy transformation, and the degree of change per unit volume is less than the error in any acceptable method of measurement.

The basic reason for the difficulty in determining the absorption coefficient accurately is that absorption is a function of wavelength, temperature, pressure, the medium, and the particle concentration. Theoretically, the absorption coefficient of distilled water under standard conditions should be constant. Unfortunately, there is wide variation in the values reported by several researchers [1]. This is believed to be due to non-standardized methods and equipment.

The total absorption coefficient, a, can be obtained by using Equation (2); the attenuation coefficient, α, is obtained with Equation (1), since the measurement of attenuation is not difficult, basically. Several instruments have been devised for this purpose [22]. The scattering coefficient, S, is determined through separate measurement.

1.2.3 Light Scattering

As light energy passes through a medium, it encounters many particles of the fluid (i. e. suspended particles, molecular structure of the medium, etc.). According to Haltiner and Martin, some of the particles (dipoles) may have centers of positive and negative electric charge displaced one from another [10]. The dipole will vibrate sympathetically at the frequency of the incident electromagnetic energy. The result is that the particle radiates light energy in all directions.

Attenuation is a function of the wavelength of the incident light energy. Duntley and Koslyaninov show, for a wavelength of 480 millimicrons (i.e. visible blue light) with a collimated incident beam, approximately 60 percent of the attenuation can be attributed to scattering and 40 percent to absorption [24, 27]. This choice of monochromatic wavelength is discussed by Tyler, et. al., as being in the band of minimum absorption by distilled water [24, 25]. This band is bounded by 480 millimicrons for distilled water and approximately 590 millimicrons for coastal sea water. In addition to its variation with wavelength, light attenuation also varies with scattering and absorption as already discussed. The authors have used monochromatic or limited wavelength band incident light so as to minimize the variation of attenuation.

Absorption by the particulate material in sea water is small, and may be ignored according to Tyler [11, 24]. The variation of absorption with temperature and pressure can be eliminated by using constant temperature, at one atmosphere, in a laboratory-controlled experiment, and comparing these results with in situ measurements. This procedure reduces the variation of the scattering phenomenon.

Some scattering (see Figure 1) is the result of the incident energy encountering the medium itself. It can be considered molecular scattering and is described by Rayleigh theory. Duntley indicates that molecular scattering is of equal magnitude in the forward and backward directions for a collimated light source in sea water [27]. He also states that molecular scattering accounts for about seven percent of the total

observed scattering. This means that the molecular scattering is generally several orders of magnitude smaller than particle scattering, in the forward direction.

The establishment of a specific total volume scattering coefficient is also a complex problem, but it can be measured directly. Consideration must be given to the incident energy wavelength as well as to the particle size, particle concentration, and energy dispersion. Total scattering is defined by the following functions:

$$\sigma(\theta) = J(\theta)/HV(\theta) \; ; \qquad (3)$$

$$S = 2\pi \int_0^{\pi} \sigma(\theta) \sin\theta \, d\theta; \qquad (4)$$

θ is the angle at which the intensity is measured relative to the source axis, $J(\theta)$ is the intensity measured at the angle θ, H is the input intensity per unit area, and $V(\theta)$ is the unit volume determined by the beam volume and the subtended receiver surface area. The units of $\sigma(\theta)$ are length^{-1} (see Figure 2).

1.2.4 The Effect of Particle Size, Particle Concentration and Wavelength on Scattering

The Mie theory of scattering states that scattering is a function of particle size, r, and incident energy wavelength, λ [19]. These two parameters may be related in terms of a parameter, B, as in Equation (5):

$$B = \frac{2\pi r}{\lambda} \qquad (5).$$

When scattering particles are large in comparison to wavelength, ($B \geq 8$), the scattered intensity is a complex function of the incident energy wavelength, relative index of refraction of the scatterers, and the angle of measurement. The relationship of these factors is described by the Mie theory, and varies as ($\lambda^{-\gamma}$). The exponent γ takes on values which range from zero for distilled water to four or five for very turbid water [19]. Values of the theoretical function B are available, tabulated by the Bureau of Standards et. al. [2, 3, 12].

For particles comparable in size to the wavelength, the scattering function decreases in complexity, and is described in tables of the functions as indicated above. When the scattering particles are much smaller than the incident light wavelength ($B << 1.0$), the relationship reduces to the simpler Rayleigh theory. In all of the scattering theory for $B > 1$, the use of polarized source light reduces the complexity of function computation.

When B has a large value, the resulting scattering curves show a preponderance of forward scattering, as noted in Section 1.1. As B decreases, the scattering pattern becomes more nearly symmetrical about the intercepted volume, and is symmetrical for molecular (Rayleighen) scattering. When considering the light intensity change in a scattering medium due to scattering only, the turbidity or fractional decrease in intensity is written as

$$N_r / N_o = e^{-K\pi r^2 n l} \qquad (6).$$

In this relationship, n is the number of particles per unit volume; K is a function of B and the relative index of refraction, m; r is the particle radius; and l is the path length traveled by the transmitted energy. Thus, for very small (molecular) particles:

$$N_r/N_o = \frac{16\pi^4 r^6 (m^2-1)}{\lambda^4 l\,(m^2+2)}(1+\cos^2\Theta) \qquad (7).$$

Integration over all values of Θ and substitution into Equation (6) results in the following expression:

$$N_r/N_o = e^{\left[\frac{-128\pi^6 r^5}{3\lambda^4}\left(\frac{m^2-1}{m^2+2}\right)^2\right] n l} \qquad (8).$$

The variation of K for values of m and B is shown in Figure 3.

If light transmission were to be measured through a system of randomly dispersed particles, it would be best to select a wavelength where absorption is minimum and lessen the complications for evaluation of light scattering. If, on measuring the decrease in intensity, the intensity is found to vary as γ^{-4}, minimum absorption could be assumed. However, the generally accepted method for computing absorption is by calculating the difference between total attenuation and total scattering.

There is no complete theory at this time to treat large, irregularly shaped particles; however, most shapes can be reasonably approximated by spheres if the particles are not too large.

1.3 Station Oceanographic Climatology

The authors feel that an oceanographic climatological

survey is required to describe the sampling area and to be certain that measured values of temperature and salinity are valid.

We have prepared a brief description of the sampling area. The data used were those for which turbidity measurements were available. The description presented is from data obtained from oceanographic field sheets covering a four-year period (1951-1955) at Hopkins Marine Station of Stanford University in Pacific Grove, California. The data were processed and analyzed with the BMDX-13 statistical accumulation and correlation program on the USNPGS CDC-1604 computer.

Temperature and salinity were analyzed as to depth and month. The results are presented in Table 1 for the months during which the field sampling was performed. The extinction coefficient data given (Figure 4) are for the entire climatological sample rather than the months of the field work.

Figure 4 shows the temperature and salinity profiles for December, January, February and March, and the same data median values are shown in Table 1.

January shows the weakest vertical temperature gradient as a result of the more intense winter stirring and the warm northward flowing Davidson Current. Not shown in Figure 4, but in the analysis of the entire five-year sample, is a vertical temperature gradient of two degrees Celsius in the fifty-meter surface layer.

A well-mixed surface layer is shown for December and January only, and a weak salinity gradient is evident for this

period as well.

An investigation of light attenuation versus cloud cover was conducted; first, to determine the validity of the observations; and second, to determine the shape of the extinction curve in the vertical at the chosen location. 107 observations made with an hydrophotometer were available. Two values were available for each observation; one for incident sunlight at the sea surface, and one for light existing at each depth.

A small negative correlation (0.16) was found between the surface light and cloud cover. Whether this correlation should be this small or if it should be larger is difficult to say, as there is certainly some light even with overcast skies. There is also the possibility of large observational error here, because of variability in observational technique.

The next step in the light investigation was an examination of light versus depth. This gave a negative correlation of 0.69. Figure 5 is a graph of relative radiance (relative to incident insolation at the surface) by depth, using the 155 available observations. Figure 5 shows that the relative radiance approaches zero as depth increases, and allows some quantitative comparison. Curve 1 of Figure 5 is a plot of percent of incident sunlight versus depth, measured by Tyler in 1957 with a photometer oriented at the zenith angle in fresh water, and the sun at 65° altitude [11]. Curve 2 is a similar plot for the data of the present study, which was hand-fitted to extinction hydrophotometer data. The observations were made at 10:30 a.m. ± 30 minutes, so it is safe to assume that the sun altitude was not much different

from 65°. Aside from the variation due to sun altitude, there are unknown instrument differences, and the data available were not of the precise nature of Tyler's data. These factors, along with the difference in water type, contribute to the difference of the slope of curves 1 and 2. Curve 3 is hand-fitted to the station climatological turbidity data. It is observed from the curves of Figure 5 that Monterey Bay water is relatively turbid.

Here, we can point out that a very shallow thermocline such as exists in the Bay water would hold the more turbid water close to the surface, and tend to change the radiance curve in the manner noted in Figure 5 for this study. This turbidity appears to be concentrated in the upper 25 meters, as there is practically no radiance below 25 meters as indicated by curve 3.

Another contributing factor in this regard is the difference in incident sunlight. In the present investigation, the mean incident cloud cover for the 155 observations is 53 percent, while Tyler's curve was established in a single clear day.

The resulting conclusions as to radiance of Bay water is that in the vertical, total extinction is similar in many respects to Tyler's data, but that the water is relatively more turbid in the upper 25 meters [11].

2. Equipment Description

2.1 Sea Water Attenuation Hydrophotometer (Alpha Meter)

This instrument was supplied by the Visibility Laboratory of Scripps Institute of Oceanography, San Diego, California. It is designed to measure total horizontal light attenuation. It consists of a constant light source with a monitor cell in a sealed container on one end of a three inch I Beam, as shown in Figure 6. On the other end of the bar is a photocell, also enclosed in a watertight container, with a Wratten Filter number 57. The electric power is supplied on board the USNPGS Hydrographic Research Vessel by two 500-kilowatt generators. The control box contains two potentiometers to display transmitted and received intensity. The Alpha Meter is first standardized in air to calibrate the two meters with the power supply. Then the apparatus is lowered just below the sea surface and is standardized at this position and the first reading is made. Since this meter determines horizontal light attenuation, attention must be given to maintaining a horizontal position during all readings. Lowering the Alpha Meter to specific meter wheel depth readings allows data to be taken at depths down to a maximum cable length of 50 meters.

The Wratten Filter number 57 passes maximum intensity at 0.5364 microns with a half width of 0.050 microns. This band is in the region of maximum transmittance of light in sea water. Forward angle scattering was measured using light in the same wavelength band.

2.2 Insolation Extinction Hydrophotometer, G. M. Mfg. & Instrument Corp. Submarine Photometer Model 15M04

This instrument was used to determine solar radiation extinction with depth, which gives a measure of upper layer turbidity. The basic equipment, as shown in Figure 7, consists of two photocells; one, a deck monitor to measure surface incident solar radiation, the second to measure solar radiation at some selected depth. The information is displayed by means of two potentiometers mounted in the deck control box. This allows the operator to obtain significant data points at pre-selected depths, and to determine the depth at which solar radiation is totally attenuated. A Wratten Filter number 57A is used with the in situ photocell, which has a peak transmittance at a wavelength of 0.5340 microns and a half width of 0.060 microns, which overlaps the band width of the Alpha Meter Wratten Filter number 57.

With the Insolation Extinction Hydrophotometer and the Sea Water Attenuation Hydrophotometer, it is possible to obtain vertical and horizontal attenuation in the upper layers simultaneously. There should be an extinction maximum in the areas of high concentration of particulate matter. It is also possible to compare these data with other oceanic areas, as will be seen later.

2.3 Scattering Analysis Apparatus

2.3.1 Constructed Laboratory Model

As shown in Figure 8, there are four major components to this variable angle scattering analysis apparatus: a Mercury Arc lamp; and Eldorado Differential Photometer, Model 210,

with two photocells, (capable of recording as small as two micro-micro lumens); a Leeds-Northrup Analog Chart Recorder; and the variable angle protractor scattering table with one liter flask, aperture, wavelength discrimination filter, polarization neutral screen, and focusing (collimation) lens.

The Mercury Arc lamp produces a narrow beam which contains monochromatic lines at 0.6907, 0.6234, 0.5791, 0.576959, 0.5461, 0.4960, 0.4916, 0.435835, and 0.404656 microns. The lines at 0.576959, 0.435835, and 0.404656 microns are the only lines whose intensity are of practical use. Using a Wratten Filter number 57, it is possible to eliminate all the lines except the desired wavelength of 0.576959 microns.

It is desirable to collimate the beam to eliminate any beam divergence over the measuring path. This can be done by using a 3/32 inch aperture with a five-inch focal lens. Proper alignment and positioning of aperture and lens gives nearly zero divergence over the path used (beam width is 0^{o}-8' at the receiver). A pair of adjustable polarizing lenses are positioned in the beam to obtain control of the absolute intensity which is received by the Eldorado Differential Photometer photocells. The flask is positioned over the center of the protractor scattering table with its relative position always checked for consistancy to eliminate any changes in beam path due to glass-water interface refraction.

One of the photocells is positioned on the beam path. The second is secured to the rotating arm of the protractor scattering table. An electric slow speed AC motor is geared to the rotating arm so as to provide the necessary constant

rotation of the variable position photocell. The arm movement is slow enough to present a useful curve on the Leeds-Northrup Analog Recorder, giving readings on a continuous curve rather than at discrete points.

To align the apparatus, it is necessary to diminish the signal received by the fixed arm photocell to a value which allows adequate scale freedom on the Eldorado Differential Photometer. Alignment is then made with the air-filled flask to eliminate flask refraction effect. This is repeated with distilled water, so that the ultimate data will be relative to the distilled water.

As is seen in Figure 9, this apparatus can process a large number of one liter samples in complete darkness, with a permanent record of the results. The product is a continuous curve of scattering at angles varying from that perpendicular to the beam axis to along the axis.

2.3.2 Aminco Light Scattering Microphotometer

The Aminco Microphotometer, of the American Instrument Company, Inc., Silver Spring, Maryland, was used for samples of less than one-liter volume and for individual point studies (i.e. at particular angles). The apparatus, shown in Figure 10, consists of the same general components on the larger scattering apparatus with the exception of not having a differential photometric capability. The same type AH4 mercury arc lamp is the light source with a Wratten 57 Filter and a three-inch focal length collimating lens. The receiver photocell which sits on a variable-angle plate receives and displays the intensity of light scattered from the sample at various angles with respect to the light beam. The apparatus gives good small-angle forward scattering resolution for a 62.8 cubic-centimeter sample, but because of the necessity to pre-position definite angles manually, and the sample size limitation, it was used as an auxiliary and checking system.

The procedure is to determine the light beam intensity first in air, and then with a sample of distilled water at each degree relative to the beam axis. When this calibration is complete, any sample can be investigated at any angle desired. After completion of sample analysis, another distilled water sample is analyzed for beam attenuation on the axis to evaluate the meter drift.

2.4 Salinity Determination Apparatus

The Hytech Model 621 Inductive Salinity and Conductivity Meter was used to measure salinity. The Meter uses

the magnetic induction method to compare the conductivity of a sample with that of Copenhagen water. This apparatus compensates automatically for temperature differences between the sample and the standard; if the differences are small, allowing all reagents to come to room temperature will satisfy the temperature requirements. The salinity range capability of the Meter is from 0 to 44°/oo with an accuracy of 0.003 percent salinity, which includes errors which may be made during normal handling procedures using a 50 cubic centimeter sample.

2.5 Phosphate Determination Apparatus

The phosphate determination was conducted using a color comparison technique with the Beckman DU Spectrophotometer. The Spectrophotometer compares a sample, after the addition of an acidic solution of ammonium molybdinate, plus an agent such as stannous chloride to reduce the complex phosphomolybidic acid to a blue colored substance, with a prepared set of samples of known concentration. This colorimetric quantitative analysis determines differences in the colors which are proportional to the concentration of the phosphate in the sea water sample. The accuracy of the results is about 5 percent throughout the phosphate concentration range, which generally lies between 0.00 and a maximum of 3.00 milligrams per liter for sea water.

3. Procedure

3.1 Sample Collection and Attenuation Measurement

The primary purpose of this investigation is to discover the nature of the vertical variation of light scatterers in Monterey Bay. Previous work in this field has pointed toward a need to analyze forward-angle scattering, and the techniques and apparatus were designed with this in mind.

Working on a foundation of information published by Burt, Tyler, et. al., the authors concluded that uncontaminated water samples collected in the field would retain their optical properties if analyzed quickly enough to preclude decomposition of suspended organic matter, and they could be collected by Nansen bottle cast [9, 17, 22, 23]. Spilhaus showed, in his study of the areal distribution of scattering, that it was practicable to use a shipboard laboratory device to measure scattering in samples collected by Nansen bottle cast [35].

Sample depth was determined by a combination of wire-angle computation and bathythermograph slide interpretation.

The water samples were collected on 21 December, 1964: 6 and 8 January, 26 January, and 19 February, 1965. The first three days were during a stormy weather period and the surface waters were well-mixed. The last two days were during a relatively calm period and the surface water mixing was less intense. The spread of collection days was due to severe weather conditions.

A station was selected offshore on the rim of the Monterey Submarine Canyon in about 900 fathoms of water. This station was chosen because of its location at the Bay entrance,

with expected low terrestrial polution. Also, previous sunlight extinction data were available for comparison, and the oceanographic climatology of the area had been established (note Section 1.3). This station is located at 36°42'N and 122°02'W, and all samples were taken within two miles of this location, with positioning by visual bearings (see Figure 11).

Three types of light transmission measurements were made:

(a) horizontal attenuation of a light beam, in situ, using the Alpha Meter (Figure 6).

(b) vertical extinction of sunlight, using the hydrophotometer in situ (Figure 7).

(c) horizontal scattering of a collimated light beam, with scatterometers in a shore laboratory, shown in schematic form in Figure 2.

All light measurements were made at nearly the same wavelength. The procedure at the Bay station was:

1. Horizontal attenuation measurement at five-meter intervals to cable limit.
2. Sunlight extinction measurement at five-meter intervals.
3. Nansen cast at standard depths.
4. Bathythermograph cast.

Immediately upon returning to port, the water samples were taken to a USNPGS laboratory for scatterometer measurement. Later, the salinity and phosphate determinations were made, with careful handling of samples and storage at a constant 66° F temperature.

3.2 Forward Angle Scattering Measurement

All scatterometer readings were preceded by readings with the chamber first air-filled for meter calibration and then filled with distilled water to provide relative values for Mie scattering determination. Individual readings for air, distilled water, or sea water, consist of a base transmission reading made with a cell on the beam axis to check alignment and intensity and a curve of scatterometer readings from angles of 90° to 180° relative to the beam axis.

To establish the vertical variation of suspended material, as many variables as possible must be eliminated. This may be accomplished by:

1. Selection of a narrow wavelength band (approximately monochromatic) to assure minimum absorption (by wavelength selection) and eliminate variability of Rayleigh scattering. The most effective wavelength has been found to be .56 microns, for bay water. A comparable wavelength value for turbid coastal water is close to 0.58 microns, and for distilled water, about 0.48 microns. Natural sea water acts as a monochromator in this region, with minimum absorption generally near a wavelength of 0.53-0.54 microns. Available data for comparison of results and standardization can be used if a monochromatic light source is used [11, 24, 35].
2. Collimation of the light source to assure predominance of forward scattering and placing

the scattering dependence on scatterer size and concentration.

In the scattering apparatus, $\sigma(\theta)$ was measured at angles and plotted as relative signal intensity versus angle. The position of the curve for each sample should provide a large particle scatter coefficient. Comparison of slopes of the curves should give an indication of particle size distribution. This assumes the Rayleigh scattering is constant from sample to sample, and is the same for either distilled or sea water.

In line with Tyler's paper on angular resolution in scattering measurement, a beam of high collimation with vertical receiver slits was used in scattering measurements [26].

4. Data

4.1 Light Attenuation Data

Data shown in Table 2 were taken by means of the Scripps Alpha Meter, as outlined in Sections 2.1 and 3.1, and were observed *in situ*. The difficulties encountered were due to the large wire angle caused by existing weather conditions. This caused the cable weight to be exerted on the pressure connectors of the cables. This additional weight, plus the boat motion, brought about occasional cable separation. On the 8th of January, the wire angle was zero and the cable parted at the connectors due to cable weight and handling. On the 26th of January, the cable developed an internal break at a splice point, making data-taking impossible. On the 19th of February the apparatus operated perfectly.

4.2 Light Extinction Data

Data shown in Table 3 were obtained *in situ*, using the USNPGS Solar Radiation Extinction Hydrophotometer, described in Sections 2.2 and 3.1. The first two cruises were late in the day and the weather was bad, with high winds and heavy cloud cover, and this gear was not used. The next two cruises had good weather conditions and the resulting data were taken at mid-day on both days, at about 1415 local time. On the 19th of February the apparatus was lowered just as the boat drifted into a fog bank which decreased the amount of incident radiation. On this day the water was extremely turbid.

4.3 Scattering Coefficient, Density, Phosphate, Particle Concentration Data

Data shown in Table 4 were taken in a USNPGS laboratory with equipment and procedures explained in Sections 2.3, 2.4, 2.5, and 3.2. The scattering data were first taken on a table arrangement shown in Figure 8. The procedure was awkward because the measurements had to be made in the dark. A constant speed drive was necessary to give the required constant angular velocity for the scattering measurements. Difficulties arose because the scattering intensity varied through three orders of magnitude, requiring the shifting of meter scales at the correct moment, in total darkness. If time were available to correct the design of this scattering apparatus, the present undesirable features could be eliminated. It might prove to be a most accurate scattering measuring device because of the high sensitivity of the differential photometer.

The samples obtained on the 26th of January and the 19th of February were analyzed, using the Aminco Scattering meter described in Section 2.5. The Aminco Meter is less sensitive than the constructed protractor table. This drawback is more than compensated for by the use of small samples, working in a lighted room, and measurement at discrete points rather than continuously.

A plot of the scattering function $\sigma(\theta)$ versus angle has a distinctive shape, (see Figures 12, 13, and 14). The shape of this curve is controlled by the particle size, and the area under the curve is proportional to the concentration of the scatterers. The National Bureau of Standards, et. al. have

published tables of the scattering function $\sigma(\theta)$ and a related value K, ($K = S/B^2$) for many combinations of the parameters of particle size $\left(B = \frac{2\pi r}{\lambda}\right)$ and relative refractive index m [2, 3, 12].

The tables of $K(m,B)$ are based on concentrations of one particle per unit volume of liquid medium. The $\sigma(\theta)$ values mentioned above were computed by evaluation of the Mie scattering equations. The curves showing the theoretical values are shown in Figures 12, 13 and 14. The Mie curves for the Nansen bottle samples (shown in Figure 15) are similar to the theoretical curves mentioned above, in shape.

A segment-by-segment integration of the measured scattering using Equation (4), shows that approximately 75 percent of the volume scattering coefficient is achieved in the angles from the beam axis between 160° and 180° [35]. This is also the region where the large particle scattering effect is greatest (see Section 1.2.3). Using large plastic overlays of Figures 12, 13, and 14, it was possible to match the measured curve slopes from 179° to 160° to the theoretical single-particle curves. This provided an estimate of particle size and relative refractive index for each sample curve.

5. Data Interpretation

The values of scattering intensity and volume scattering coefficient are shown in Table 4. Using these data, the vertical variation of the volume scattering coefficient, the relationship between the scattering coefficient and sea water density and inorganic phosphate, and the approximate size and concentration of suspended particulate matter can be determined.

There is a reliance on certain established facts and assumptions. Two fundamental ideas are: 1. absorption in sea water is minimum for collimated light; 2. the best wavelength band for coastal water transmission is .48 to .59 microns, (see Section 1.2). The wavelength used in this study is .5364 microns.

The assumptions which were used are:

1. Scattering by particles small compared to the wavelength is negligible.
2. Scattering is constant for distilled water at a constant temperature, for a particular water sample.
3. The large particles are assumed to be of homogeneous composition and similar to one another in chemical and physical makeup, and consequently, have the same relative refractive index.
4. Absorption by suspended matter is small relative to scattering.
5. Particles in each sample are assumed to be uniformly sized and uniformly dispersed.

6. Scatterers will remain in suspension and unchanged for a short time (about four hours) after sample collection.

It is believed that most of the material found in sea water of the particular size under investigation has a relative refractive index in the range 1.2 to 2.0, particularly the organic material.

On the last sampling day, the bottom two bottles picked up samples from a turbidity current along the canyon wall. Upon retrieval, the bottom weight was dragged along the canyon wall and a small sample of mud and pebbles was obtained. It was felt that a sediment analysis of this sample would give an indication of the nature of the suspended material in the sea water above. The analysis of the bottom sample by Lieutenant Gordon Monteath showed over two-thirds of the sample to be in the size range of less than 12.5 microns (percent by weight) [36]. The material was a greenish-brown, very fine silty sand matrix, surrounding well-rounded pebbles of granodiorite and quartzite. Over 60 percent of the sample was quartz and feldspar (75 percent of this was light pink in color and in the size range less than 12.5 microns). There were notable amounts of mafic minerals, shell fragments, biotite, and aggregates-coprolites.

The majority of these minerals and other substances have an index of refraction which is in the range 1.20 to 1.65. Therefore, the use of m values between 1.20 and 1.44 seems to be appropriate in this study. Referring to the K-field chart, Figure 3, the relationship can be seen between $K(m,B)$,

(which is proportional to volume scattering), particle size, r, and the index of refraction, m. This chart shows that the larger particles (which most affect the scattering) have an m range between 1.20 and 1.44. The region of maximum K value (for $B<12$) is found in a zone of decreasing B values and increasing m values. As the index of refraction increases, the greatest scattering (greatest K) is found to be associated with particles of smaller and smaller radius.

After the selection of the appropriate B and m values for each sample curve, a plot of the theoretical K-field was entered and the applicable K value was determined. Using Equations (1) and (2) and assuming absorption to be negligible gives

$$N_r/N_o = e^{-S\ell} \qquad (9).$$

Setting Equation (9) equal to Equation (6) gives

$$S = K\pi r^2 n \qquad (10).$$

The measurement of scattering intensity, $J(\theta)$, and solution of Equation (3) and Equation (4) gave us a measured value of S. We have a fitted K and an estimated r value (determined from $B=\frac{2\pi r}{\lambda}$, Section 1.2). Solution of Equation (10) for each sample gives a measure of particle concentration n. These are shown in the data compilation, Table 4.

Concentration is seen to be proportional to scattering and inversely proportional to particle size. Values shown in Table 4 for the two parameters, radius and scattering coefficient, were obtained by different means.

Figure 21 shows a scatter diagram of S versus n, according to particle radius. There appears to be a separation in the relations for particle size of one to two microns and those greater than two microns. Except for very small particles, scattering increases with particle radius for a given concentration. This relationship is more pronounced for the one to two micron size than for particles larger than two microns. It is also shown in the K-field (Figure 3) that the K value increases for increasing particle radius, in the size range of interest (greater than one micron).

An examination of the particle size variation shows no clear relationship with depth, considering all samples. Particle sizes obtained from curve fitting are mainly in the size range between 1.6 and 2.4 microns. The reader will note from Figures 16 to 20 that a definite difference in vertical profiles of salinity, phosphate, and sigma t exists for the last two sample days as compared to the first three days. Weather conditions would tend to cause the upper water layers to be well-mixed on 21 December, and 6 and 8 January, while layered conditions existed on 26 January and 19 February. One would expect, then, a uniform size distribution in the upper layers for the first three sample days. Looking at particle size from the standpoint of a layered system, it was found that on the three sample days with mixing, the upper 50 meters (considered as a mixed layer) shows a more uniform particle size than is shown on the last two days. This suggests that the resulting variation in scattering in the upper layer may be due to variations in particle concentration.

Figure 22 shows the scattering field for values of particle radius and particle concentration. This empirical relationship should be verified by future experimentation.

It is difficult to say how the surface area-to-mass ratio of particles will be distributed with depth. The relative refractive index of lightweight particles with the nature of wax or animal fat would be about 1.2. The same index for mineral material such as quartz might range up to 1.5. The small index difference is considered in the curve fitting. The surface area-to-mass ratio should have wide divergence for organic and mineral particles. The computed particle sizes would lead us to believe that we should be able to detect an increase of size with depth under calm conditions. It is possible that the large particles we see are of very light material and not greatly affected by gravity. The majority of the scattering particles however, probably are not living zoo or phyto-plankton. A previous study by the authors of the most common Monterey Bay planktonic forms shows a range in size upward from 15 microns.

It was hoped that some clear relationship between scattering and phosphate concentration might be found; (see Figure 23). It is noted that there is little variation of scattering with phosphate amount for the two sample days with layering in the upper 50 meter layer (Table 4). More variation is seen below 50 meters. For the three days with mixed waters there can be seen a negative correlation between scattering and phosphate in all samples, with a tendency for greater scattering in the upper 50 meters. There is no in-

dependent verification of the latter relationship; however, some support is provided through data from the first two days (the well-mixed condition) when phosphate was observed to be high in the surface waters.

No definite conclusion can be formed concerning the relationship between particle concentration and depth. There appears to be a tendency for greater concentration of particles above 50 meters for the two days exhibiting an unmixed layer. The computed scattering coefficient is relatively large at the base of this unmixed layer.

Little useful information on scattering can be obtained from the attenuation and extinction data because of poor data overlap with the scattering analysis. A check of the data shows the resulting absorption to be reasonable when checked using the attenuation-scattering difference.

6. Conclusions

The clear relationship expected between scattering coefficients and density and phosphates did not develop from this study, although a tendency is suggested in this direction. Perhaps a future study using a much larger sample size will verify the trend. There seems to be a light scattering layer (comparable to the deep scattering layer for sound transmission) at about 50 meters. This layer appears to be partially destroyed by mixing in the upper layers from storm activity. This light scattering layer appears to be associated with the upper margin of a pynocline which would buoy small particles and organisms and tend to be a collection area for these less dense materials. Seasonal variation of this pynocline will definitely affect the optical water mass characteristic. This in turn will affect the variation of solar radiation present in the region of the pynocline. This scattering layer will also affect the variation of attenuation with depth due to increased scattering and absorption. It is possible that this layer has a high concentration of planktonic organisms which exist in the region of less than one percent incident solar radiation.

From the data (Table 4) on particle size and concentration, we conclude that the methods used are sound and the results valid. The techniques could be adapted to ship-board use for the rapid processing of a large number of samples. The final computations are, however, tedious and time-consuming and computerization of all computations after initial intensity readings is desirable.

To provide more meaningful results from future studies of this type, the authors feel that attenuation hydrophotometer measurements are necessary for all levels where samples are taken. This provides a check on the order of magnitude of scatter coefficients and any layering discovered can be closely sampled to obtain data on parameters affecting the variation of scattering. If a verification is achieved, Figure 23 would be useful for estimates of particle radius and particle concentration if a scattering coefficient is available.

In future studies the authors recommend:

1. The use of a coherent light source with variable wavelength selection.
2. The use of a monochromatic collimated light source with at least two discrete wavelength selections to give beam definition and the ability to determine particle size and concentration without the undesirable and subjective curve fitting technique.
3. A chemical and microscopic analysis be made with <u>in vitro</u> samples to be correlated with associated scattering data.

The authors wish to express their profound gratitude to Dr. Glenn H. Jung for his assistance. Without his staunch support, a problem of this magnitude could not have been completed. The technical assistance of Dr. Gerald D. Ewing in the field of light transmission in sea water is greatly appreciated. The work of Dr. Raymond L. Kelly and Professor

Sidney H. Kalmbach in optical physics; Dr. Charles F. Rowell in chemical oceanography; Richard W. Haupt, Commander, United States Navy, in oceanographic instrumentation; and Assistant Professor Warren Denner all contributed to this complex study. We wish to express our sincere thanks to Gordon Monteath, Lieutenant, United States Navy, for his sediment analysis and his assistance in sampling on 21 December, 1964, and 6 January, 1965. The weather conditions on both of these days were extreme, and without his help, the operation might have met with instrument loss before the sampling and experimentation got started. The authors wish to express their appreciation to Mr. Roswell Austin of the Visibility Laboratory at Scripps Institute of Oceanography for the use of the Alpha Meter. For the computer techniques and programming advice, we are deeply indebted to Mrs. William L. Johnson. Credit should be given to our wives, Mrs. Charles Bassett and Mrs. Harry Furminger. Their typing, editing, data breakdown and moral support was outstanding and essential.

BIBLIOGRAPHY

1. Sverdrup, H. U., Johnson, M. W., Fleming, R. H. The Oceans. Prentice Hall, Inc., 1942.

2. National Bureau of Standards. Tables of Scattering Functions for Spherical Particles. United States Government Printing Office. January, 1949.

3. Grumprecht, R. O., Sung, N. L., Chin, J. N., Sliepevich, C. M. Angular Distribution of Intensity of Light Scattered by Large Droplets of Water. Journal of the Optical Society of America, v. 42, November, 1951: 226-231.

4. Johns Hopkins University. The Dual-Filter Hydrophotometer, by J. Williams. March, 1953. Technical report number 5.

5. Davis, C. N. Survey of Scattering and Light by Particles. British Journal of Applied Physics, v. 5, Sup. 3, 1954.

6. Lewis, P. C., and G. F. Lothian. Photoextinction Measurements on Spherical Particles. British Journal of Applied Physics, v. 5, Sup. 3, 1954.

7. Johns Hopkins University. The Tri-Filter Hydrophotometer, by J. Williams. June, 1955. Technical report number 9.

8. Barum, E. G. The Ecology of Sonic Scatterers in the Monterey Bay Area, California. Dissertation, Stanford University, November, 1956.

9. Burt, W. V. On Attenuation of Light in the Sea. Journal of the Marine Biology Association of the United Kingdom, v. 36, 1957.

10. Haltiner, G. J. and F. L. Martin. Dynamic and Physical Meteorology. McGraw-Hill, Inc. 1957: 79-104.

11. Tyler, J. E. Monochromatic Measurement of the Volume Scattering of Natural Waters. Journal of the Optical Society of America, v. 47, August, 1957: 745-747.

12. Ashley, L. E. and C. M. Cobb. Single Particle Scattering Functions for Latex Spheres in Water. Journal of the Optical Society of America, v. 48, April, 1958: 261-268.

13. Clark, G. L. and R. H. Backus. Measurement of Light Penetration in Relation to Vertical Migration and Records of Luminescence of Deep Sea Animals. Deep Sea Research, v. 4, 1958: 1-14.

14. Woods Hole Oceanographic Institution. Measurement of the Spectral Distribution of Light Underwater, by C. J. Hubbard. January, 1958. Report no. 58-6.

15. Rakestraw, N. W. Particulate Matter in the Oxygen Minimum Layer. Journal of Marine Research, v. 17, 1958: 429-431.

16. Woods Hole Oceanographic Institution. Optical Studies of Particulate Matter in the Sea, by D. H. Shontig and B. H. Ketchum. February, 1958. Report no. 58-15.

17. University of Washington, Department of Oceanography. Specific Scattering by Uniform Minerogenic Suspensions, by W. V. Burt. January, 1959. Report no. 42.

18. Tyler, J. E. Natural Water as a Monochromator. Limnology and Oceanography, v. 4, January, 1959: 102-105.

19. Orr, C., and J. M. Dallavalle. Particle Size Measurement from Radiation Transmission: Fine Particle Measurement. Mac-Millan, 1959.

20. Laevastu, T., Factors Affecting the Temperature of the Surface Layer of the Sea. Sociates Scientiarum Fennica, Helsinki, 1960.

21. U. S. Naval Research Laboratory. A High Resolution Investigation of the Relative Spectral Attenuation Coefficients of Water, by L. F. Drummeter and G. L. Knestrick. May, 1961. Preliminary report no. 5642.

22. Tyler, J. E. and R. W. Preisendorfer. Transmission of Energy Within the Sea. The Sea, v. 1, Interscience, 1961.

23. Tyler, J. E. On the Measurement of the Scattering Function of the Sea. International Union of Geodesy and Geophysics Symposium on Radiant Energy in the Sea, Helsinki. Monograph no. 10, June, 1961: 40-45.

24. Tyler, J. E. Scattering Properties of Distilled and Natural Water. Limnology and Oceanography, v. 6, October, 1961: 451-456.

25. Tyler, J. E. Measurement of Scattering Properties of Hydrosols. Journal of the Optical Society of America, v. 51, November, 1961: 1289-1293.

26. Tyler, J. E. and C. Howerton. Instrument for Measuring the Forward Scattering Coefficient of Sea Water. Limnology and Oceanography, v. 7, July, 1962: 393-395.

27. Duntley, S. G. Light in the Sea. Journal of the Optical Society of America, v. 53, February, 1963: 214-233.

28. U. S. Naval Research Laboratory. Transmission of Ruby Laser Light Through Water, by J. A. Curcio and G. L. Knestrick. June, 1963. Report no. 5941.

29. Jerlov, N. G. Optical Oceanography. Oceanographic Marine Biology Annual Review, 1963: 89-114.

30. Hulbert, E. O. Optics of Distilled and Natural Water. Journal of the Optical Society of America, v. 35, November, 1963: 698-705.

31. Irani, R. R. and F. C. Clayton. Light Scattering as a Measure of Particle Size: Particle Size Measurement and Interpretation. Wiley, 1963.

32. Hopkins Marine Station, Stanford University. Pacific Grove, California. Studies of the Marine Climate and Phytoplankton of the Central Coastal Area of California, by R. L. Bolin and D. P. Abbot. July, 1964.

33. U. S. Naval Electronics Laboratory. Transparency of Coastal Waters, by R. F. Dill and A. Gargola. 1964. Report.

34. U. S. Naval Research Laboratory. Optical Properties of Materials, by G. L. Knestrick, A. G. Rockman, J. A. Curcio. July, 1964: 26-27. Progress report, problem no. N01-07.

35. Spilhaus, A. F., Jr. Observations of Light Scattering in Sea Water. Dissertation, Massachusetts Institute of Technology, February, 1965.

36. Monteath, Gordon, Lt., USN. Environmental Analysis of the Recent Marine Sediments of Southern Monterey Bay, California. Thesis, U. S. Naval Postgraduate School, 1965.

APPENDIX I

TABLE 1

MEDIAN TEMPERATURE AND SALINITY

	December		January	
Depth	Temp.	Salinity	Temp.	Salinity
0	54.18	33.06	53.46	33.11
10	54.18	33.06	53.46	33.10
20	54.17	33.06	53.47	33.23
30	54.18	33.06	53.51	33.23
40	----------		not available-	
50	52.00	33.09	53.49	33.24

	February		March	
Depth	Temp.	Salinity	Temp.	Salinity
0	52.93	33.16	51.67	32.88
10	52.75	33.24	51.57	32.95
20	52.75	33.24	51.30	32.95
30	52.54	33.24	51.28	33.01
40	----------		not available-	
50	51.51	33.29	50.02	33.12

Temperature in degrees Fahrenheit.
Salinity in parts per thousand.
Depth in meters.

TABLE 2

LIGHT ATTENUATION DATA

Meter Wheel Reading Meters	Accepted Depth Meters	Light Source Intensity Arbitrary units	Alpha Reading	Percent Transmission $e^{-\alpha}$	α	Temp. Degrees F.
21 December, 1964						
0	1	17.3	8.5	0.492	0.71	54.3
5	4.5	17.3	8.8	0.508	0.68	54.2
10	8.1	17.3	8.6	0.497	0.70	54.2
15	11.7	17.3	9.0	0.520	0.65	54.1
20	15.9	17.3	9.2	0.532	0.63	54.0
25	20.4	17.3	9.5	0.549	0.60	53.6
30	25.1	17.3	9.8	0.567	0.57	53.6
35	29.9	17.3	9.8	0.567	0.57	53.6
40	34.8	17.3	9.8	0.578	0.55	53.5
45	39.2	17.3	10.0	0.567	0.57	53.5
50	44.8	17.3	9.8	Disconnected		53.5
6 January, 1965						
0	1	15	6.0	0.400	0.91	54.5
5	5	15	8.0	0.533	0.63	52.6
10	9	15	8.0	0.533	0.63	52.6
15	13	15	8.0	0.533	0.63	52.5
20	17	15	7.7	0.513	0.67	52.5
25	22	15	8.2	0.547	0.60	52.6
30	27	15	8.5	0.567	0.57	52.6
35	32	15		Disconnected		52.5
8 January, 1965						
0	0	12	6.6	0.550	0.59	54.2
5	5	12	7.4	0.617	0.48	54.1
10	10	12	7.2	0.600	0.51	54.0
15	15	12	7.3	0.608	0.50	54.0
20	20	12	7.1	0.592	0.53	54.1
25	25	12	7.1	0.592	0.53	54.1
30	30	12	6.8	0.567	0.57	54.2
35	35	12	7.4	0.617	0.48	54.2
40	40	12	7.0	0.583	0.54	54.5
45	45	12	7.6	0.633	0.46	54.5
47	49	12	6.4	0.533	0.63	54.7
45	45	12	6.2	0.517	0.66	54.5
40	40	12	6.0	0.500	0.69	54.5
35	35	12	6.5	0.542	0.61	54.2
30	30	12		Disconnected		54.2

TABLE 2

Meter Wheel Reading Meters	Accepted Depth Meters	Light Source Intensity Arbitrary units	Alpha Reading	Percent Transmission $e^{-\alpha}$	α	Temp. Degrees F.
26 January, 1965		No readings				
19 February, 1965						
Surface	00	11.5	5.1	0.500	0.69	53.5
5	5	11.5	5.1	0.443	0.81	53.5
10	10	10.5	4.8	0.457	0.78	53.4
15	15	11.5	5.0	0.435	0.83	53.2
20	20	11.5	5.5	0.478	0.74	53.1
25	25	11.0	5.6	0.508	0.68	53.0
30	30	11.0	6.0	0.454	0.79	52.3
35	35	11.4	6.5	0.571	0.56	52.0
40	40	11.0	6.5	0.592	0.52	51.6
43.5	43	11.4	6.4	0.562	0.57	51.5
40	40	11.5	6.5	0.565	0.57	51.6
35	35	11.5	6.6	0.574	0.55	52.0
30	30	11.4	6.1	0.535	0.62	52.3
25	25	11.5	5.7	0.496	0.70	53.0
20	20	11.7	5.4	0.462	0.77	53.3
15	15	11.4	5.3	0.465	0.76	53.2
10	10	11.5	5.4	0.470	0.75	53.4
5	5	10.4	5.0	0.482	0.73	53.5
Surface	00	10.5	4.7	0.448	0.80	53.5

TABLE 3

LIGHT EXTINCTION DATA

Meter Wheel Reading Meters	Accepted Depth Meters	Source Light Intensity Arbitrary units	Trans-mittance	Coefficient of Extinction	Temp. °F	Radiance in % of Incident Sunlight
8 January, 1965						
00	00	5.0×10^2	800	1.6	54.4	100
5	5	5.5	350	0.637	54.2	39.8
10	10	5.5	220	0.400	54.2	25.0
15	15	5.5	130	0.236	54.2	14.7
20	20	5.0	70.0	0.140	54.2	8.8
25	25	5.0	40.0	0.080	54.3	5.0
30	30	5.0	35.0	0.070	54.4	4.4
35	35	5.0	21.0	0.042	54.8	2.6
40	40	4.5	12.0	0.0266	54.8	1.7
45	45	4.5	8.00	0.0178	54.8	1.1
50	50	4.8	6.00	0.0125	54.7	0.8
55	55	5.0	4.00	0.0080	54.9	0.5
60	60	5.0	2.50	0.0050	54.2	0.3
65	65	5.0	1.60	0.0032	54.7	0.2
70	70	5.0	1.00	0.0020	53.1	0.1
75	75	5.0	0.50	0.0010	52.8	0.1
80	80	5.0	0.20	0.0004	52.3	0.025
85	85	5.0	0.20	0.0004	52.1	0.025
87	87	5.0	0.0	0.000	52.0	0
00	00	5.0	750	1.5	54.4	100
10	10	4.8	220	0.458	54.2	32.4
20	20	4.3	86.0	0.200	54.2	13.3
30	30	4.4	30.0	0.0682	54.4	4.5
40	40	5.0	14.0	0.0280	54.8	1.9
50	50	5.0	6.50	0.0130	54.7	0.9
60	60	5.0	2.50	0.0050	54.2	0.3
70	70	5.0	1.00	0.0020	53.1	0.1
80	80	5.0	0.20	0.0008	52.3	0.1
87	87	5.0	0.0	0.000	52.0	0.0

TABLE 3

Meter Wheel Reading Meters	Accepted Depth Meters	Source Light Intensity Arbitrary units	Transmittance	Coefficient of Extinction	Temp. °F	Radiance in % of Incident Sunlight
26 January, 1965						
00	00	8.0×10^2	1200	1.50	54.1	100
5	5	8.0	400	0.500	54.0	33.3
10	10	8.0	200	0.250	54.0	16.7
15	15	8.0	no reading		54.0	--
20	20	8.0	54.0	0.0675	53.9	4.50
25	25	8.0	26.0	0.0325	53.9	2.20
30	30	8.0	15.0	0.01875	53.8	1.30
35	35	8.0	9.00	0.01125	53.6	0.80
40	40	8.0	5.30	0.00663	53.2	0.40
45	45	8.0	3.50	0.00438	52.8	0.25
50	50	8.0	2.20	0.00275	52.2	0.2
55	55	8.0	1.50	0.001875	51.6	0.1
60	60	8.0	1.00	0.001250	51.1	0.1
65	65	8.0	0.50	0.000625	51.0	0.04
70	70	9.0	0.40	0.000445	50.7	0.03
75	75	8.5	0.20	0.000235	50.5	0.01
80	80	8.5	0.20	0.000235	50.4	
00	00	8.0	1000	1.25	54.1	100
5	5	8.0	550	0.693	54.0	55.4
10	10	8.0	350	0.425	54.0	34.0
15	15	8.0	123	0.154	54.0	12.3
20	20	8.0	59.0	0.0738	53.9	5.8
25	25	8.0	30.0	0.0375	53.9	3.0
30	30	7.5	15.0	0.0200	53.8	1.6
35	35	7.0	8.80	0.0126	53.6	1.0
40	40	7.0	5.60	0.00800	53.2	0.64
45	45	7.0	3.50	0.00500	52.8	0.40
50	50	7.5	2.40	0.00320	52.2	0.25
55	55	8.5	1.50	0.001765	51.6	0.14
60	60	9.0	1.00	0.001111	51.1	0.09
65	65	9.0	0.60	0.000667	51.0	0.05
70	70	9.0	0.40	0.000445	50.7	0.03
77	77	8.0	0.40	0.000500	50.4	
19 February, 1965						
00	00	6.9	480	0.695	53.5	100
5	5	6.5	320	0.492	53.5	71
10	10	6.0	160	0.267	53.4	38.6
15	15	7.3	70.0	0.096	53.2	13.8
20	20	8.0	12.0	0.0150	53.3	2.2
24.5	24	8.0	0.0	0.0	53.0	0

TABLE 3

Meter Wheel Reading Meters	Accepted Depth Meters	Source Light Intensity Arbitrary units	Transmittance Arbitrary units	Coefficient of Extinction	Temp. °F	Radiance in % of Incident Sunlight
19 February, 1965						
00	00	8.0	700	0.875	53.5	100
5	5	7.0	300	0.425	53.5	48.6
10	10	5.8	182	0.314	53.4	35.9
15	15	5.5	86.0	0.156	53.2	17.8
20	20	6.5	9.50	0.0146	53.3	1.7
24.5	24	8.0	0.0	0.0	53.0	0

TABLE 4

Scattering Coefficient, Density, Phosphate, Particle Size and Concentration

Sample Number	Field Work Date	Depth Meters	Phosphate mgm. liter^{-1}	Temp. Degrees C.	Salinity °/oo	Density σ_t
1	21 Dec. '64	Sfc.	0.54	12.8	33.074	24.960
2	"	10	0.12	12.1	33.162	25.160
3	"	20	0.76	11.8	33.180	25.230
4	"	30	0.40	11.7	33.290	25.340
5	"	40	0.61	11.6	33.416	25.450
6	"	50	0.10	11.5	33.332	25.410
7	6 Jan. '65	Sfc.	0.11	12.2	33.234	25.210
8	"	25	0.12	11.7	33.304	25.350
9	"	50	0.08	11.9	33.364	25.360
10	"	75	0.18	12.0	33.356	25.330
11	"	100	0.10	12.0	33.117	25.150
12	"	125	Cloudy	11.1	33.420	25.550
13	8 Jan. '65	Sfc.	0.48	12.3	32.784	24.830
14	"	30	0.71	12.4	33.197	25.130
15	"	100	0.46	10.3	33.695	25.900
16	"	150	0.78	9.3	33.857	26.200
17	"	200	0.98	8.6	33.911	26.350
18	"	250	0.97	7.8	33.920	26.480
19	"	300	1.05	6.9	34.078	26.731
20 A	26 Jan. '65	Sfc.	0.10	12.3	33.315	25.250
21	"	10	0.28	12.8	33.372	25.190
22	"	20	0.28	12.2	33.378	25.310
23	"	30	0.28	12.1	33.638	25.530
24	"	40	0,96	11.8	33.742	25.670
25 A	"	50	0.73	11.2	33.822	25.840
26	"	75	0.73	10.3	33.639	25.860
27	"	100	0.60	10.1	33.071	26.230
28	"	150	(N.C.) 0.41 "	9.3	34.213	26.470
29	"	200	0.59	8.8	34.061	26.440
30	"	250	0.78	8.1	34.212	26.660
31	"	300	0.96	7.6	34.263	26.770

TABLE 4

Sample Number	Field Work Date	Depth Meters	Phosphate mgm. liter^{-1}	Temp. Degrees C.	Salinity °/oo	Density σ_t
32	19 Feb. '65	Sfc.	0.14	12.0	33.476	25.430
33	"	10	0.35	11.9	33.468	25.440
34	"	20	0.30	11.8	33.422	25.420
35	"	17.5	0.43	12.0	33.467	25.420
36 A	"	30	0.42	11.3	33.569	25.630
37	"	40	0.59	11.1	33.582	25.670
38 B	"	30	0.51	11.3	33.665	25.700
39	"	43	0.83	10.8	33.702	25.820
40	"	54	0.32	11.0	33.477	25.610
41	"	75	0.71	10.9	33.506	25.650
42	"	92	0.52	10.6	33.561	25.750
43	"	105 (bot.)	4.70 **	10.5	33.826	25.970
44	"	110 (bot.)	2.35 **	10.6	33.993	26.080
45 B	26 Jan. '65	Sfc.	Short ***	12.3	Short	----
46 B	"	50	Short ***	11.2	Short	----

* (N. C.) Not conclusive, solution turned yellow.

** (bot.) Bottle contained sediment.

*** Short Not sufficient sample available to perform analysis.

TABLE 4

Sample No.	Attenuation Coefficient α	Extinction Coefficient	$\beta = \frac{2\pi r}{\lambda}$	Particle Mean Radius (r) (microns)	Relative Refractive Index (m)
1	0.710		27	2.36	1.26
2	0.700		27	2.36	1.26
3	0.630		--	----	----
4	0.570		19	1.66	1.26
5	0.550		21	1.84	1.26
6			21	1.84	1.26
7	0.910		19.6	1.72	1.26
8	0.600		26	2.28	1.33
9			26	2.28	1.33
10			32	2.80	1.25
11			--	----	----
12			--	----	----
13	0.590	1.60000	32	2.80	1.25
14	0.570	0.07000	32	2.80	1.25
15			22	1.93	1.33
16			22	1.93	1.33
17			22	1.93	1.33
18			22	1.93	1.33
19			26	2.28	1.26
20 A		1.50000	17	1.99	1.26
21		0.25000	22	1.93	1.25
22		0.06750	22	1.93	1.25
23		0.01875	22	1.93	1.25
24		0.00663	27	2.36	1.33
25		0.00275	17	1.49	1.26
26		0.00023	27	2.36	1.26
27			22	1.93	1.33
28			16	1.41	1.33
29			22	1.93	1.25
30			16	1.41	1.26
31			22	1.93	1.25
32	0.690	0.69500	21	1.84	1.25
33	0.780	0.26700	5	0.49	1.25
34	0.740	0.01500	21	1.84	1.25
35	0.830	0.09600	13	1.11	1.24
36 A	0.790		5	0.44	1.25
37	0.520		5	0.44	1.25
38 B	0.620		27.5	2.35	1.33
39	0.570		22.0	1.88	1.33
40			30	2.64	1.20
41			21	1.84	1.25
42			27	2.36	1.26
43			32	2.80	1.33
44			8	0.70	1.25
45 B		1.50000	21	1.79	1.33
46 B		0.00275	25	2.13	1.33

TABLE 4

Sample Number	Volume Scattering Coefficient Meter^{-1} (S)	Concentration Particles Per cm^{3}x10^4
1	0.2179	3.11
2	0.3123	4.46
3	Short	----
4	0.2367	10.3
5	0.1794	6.04
6	0.4018	13.5
7	0.6466	27.5
8	0.8401	15.4
9	1.2020	22.1
10	0.4194	10.0
11	Short	---
12	Short	---
13	0.7649	8.32
14	0.4463	5.40
15	0.3714	13.3
16	0.1301	4.63
17	0.1778	6.33
18	0.3078	11.0
19	0.2288	3.62
20 A	0.9990	44.8
21	0.9646	25.8
22	0.9658	25.8
23	0.9579	25.6
24	0.9664	16.6
25	1.0010	44.9
26	0.0917	1.57
27	0.9252	23.7
28	0.0960	4.27
29	0.8854	21.0
30	0.8512	42.6
31	0.9271	24.8
32	0.3642	10.7
33	0.3456	202
34	0.3286	11.0
35	0.3332	17.5
36 A	0.3317	194
37	0.3363	197
38 B	0.3315	5.53
39	0.3379	12.7
40	0.3919	3.35
41	0.3109	10.4
42	0.3484	4.87
43	0.4143	3.53
44	0.5113	7.15

TABLE 4

Sample Number	Volume Scattering Coefficient Meter^{-1} (S)	Concentration Particles Per cm^{3}x10^4
45 B	0.9491	39.2
46 B	1.0031	21.9

TABLE 5

MEASURED SCATTERING INTENSITY DATA

Angle	Sigmatheta	Logsigtheta	Sample
7*			1
179.00	309.95671	5.73643	
170.00	20.64516	3.02748	
160.00	29.99999	3.40120	
150.00	25.71429	3.24705	
140.00	26.66667	3.28341	
130.00	24.54545	3.20053	
120.00	20.00000	2.99573	
6			2
179.00	311.68831	5.74200	
170.00	29.03226	3.36841	
160.00	45.55556	3.81893	
150.00	45.71429	3.82241	
140.00	44.99999	3.80666	
130.00	32.72727	3.48821	
6			4
179.00	303.03030	5.71383	
170.00	46.12903	3.83144	
160.00	35.55556	3.57110	
150.00	29.28571	3.57710	
140.00	29.16667	3.37303	
130.00	24.54545	3.20053	
7			5
179.00	265.80087	5.58275	
170.00	29.03226	3.36841	
160.00	45.55556	3.81893	
150.00	38.57143	3.65251	
140.00	60.00000	4.09434	
130.00	16.36363	2.79506	
120.00	10.00000	2.30259	
7			6
179.00	309.95671	5.73643	
170.00	29.03226	3.36841	
160.00	29.99999	3.40120	
150.00	32.14286	3.47019	
140.00	30.00000	3.40120	
130.00	74.54545	4.31141	
120.00	40.00000	3.68888	
6			7
179.00	366.23377	5.90327	
170.00	56.12903	4.02765	
160.00	57.77778	4.05660	
150.00	46.42858	3.83792	
140.00	62.50000	4.13517	
130.00	79.09091	4.37060	

* Number of data points for each sample.

TABLE 5

Angle	Sigmatheta	Logsigtheta	Sample
6			8
179.00	300.86580	5.70666	
170.00	119.03226	4.77939	
160.00	193.33333	5.26442	
150.00	232.85714	5.45043	
140.00	108.33333	4.68521	
130.00	79.09091	4.37060	
6			9
179.00	348.48485	5.85359	
170.00	140.32258	4.94394	
160.00	241.66667	5.48756	
150.00	232.85714	5.45043	
140.00	217.50000	5.38220	
130.00	118.18182	4.77222	
6			10
179.00	309.95671	5.73643	
170.00	56.12903	4.02765	
160.00	84.44444	4.43609	
150.00	92.85714	4.53106	
140.00	72.50000	4.28359	
130.00	39.09091	3.66589	
7			13
179.00	290.90909	5.67301	
170.00	72.25806	4.28024	
160.00	101.11111	4.61622	
150.00	100.00000	4.60517	
140.00	81.66667	4.40265	
130.00	76.36364	4.33551	
120.00	77.77778	4.35386	
5			14
179.00	261.03896	5.56467	
170.00	58.70968	4.07260	
160.00	78.88889	4.36804	
150.00	40.00000	3.68888	
130.00	50.90909	3.93004	
6			15
179.00	290.90909	5.67301	
170.00	45.16129	3.81024	
160.00	62.22222	4.13071	
150.00	70.00000	4.24850	
140.00	46.66667	3.84303	
130.00	38.18182	3.64236	
5			16
179.00	261.30896	5.56570	
170.00	36.12903	3.58710	
160.00	46.66667	3.84303	
150.00	30.00000	3.40120	
140.00	11.66667	2.45674	

TABLE 5

Angle	Sigmatheta	Logsigtheta	Sample
6			17
179.00	273.16017	5.61006	
170.00	40.32258	3.69691	
160.00	54.44444	3.99718	
150.00	50.00000	3.91202	
140.00	35.00000	3.55535	
130.00	12.72727	2.54375	
5			18
179.00	254.97835	5.54118	
170.00	45.80645	3.82442	
160.00	62.22222	4.13071	
150.00	59.99999	4.09434	
140.00	35.00000	3.55535	
5			19
179.00	139.39394	4.93730	
170.00	49.67742	3.90555	
160.00	69.44444	4.24053	
150.00	59.99999	4.09434	
140.00	23.33333	3.14988	
18			20
179.00	184.09425	5.21545	
178.00	85.79410	4.45195	
177.00	61.34970	4.11659	
176.00	51.02040	3.93223	
175.00	35.17315	3.56028	
174.00	22.04970	3.09330	
173.00	20.71430	3.03082	
172.00	21.17940	3.05303	
171.00	20.00000	2.99573	
170.00	20.97505	3.04333	
160.00	30.13395	3.40565	
150.00	42.20780	3.74261	
140.00	54.62185	4.00043	
130.00	61.90475	4.12560	
120.00	71.42855	4.26870	
110.00	77.38095	4.34874	
100.00	81.16885	4.39653	
90.00	92.85710	4.53106	

TABLE 5

Angle	Sigmatheta	Logsigtheta	Sample
18			21
179.00	331.36966	5.80323	
178.00	149.64086	5.00824	
177.00	105.17090	4.65559	
176.00	68.02721	4.21991	
175.00	37.87879	3.63439	
174.00	22.67080	3.12108	
173.00	20.00000	2.99573	
172.00	18.68771	2.92787	
171.00	20.47619	3.01926	
170.00	19.84127	2.98776	
160.00	29.01785	3.36791	
150.00	42.20779	3.74260	
140.00	54.62185	4.00043	
130.00	59.52381	4.08638	
120.00	65.93406	4.18866	
110.00	74.40476	4.30952	
100.00	81.16883	4.39653	
90.00	89.28571	4.49184	
18			22
179.00	349.77908	5.85730	
178.00	153.63128	5.03456	
177.00	89.83348	4.49796	
176.00	65.59767	4.18354	
175.00	43.29004	3.76792	
174.00	25.15528	3.22507	
173.00	21.07143	3.04792	
172.00	19.51827	2.97135	
171.00	20.95238	3.04225	
170.00	20.97505	3.04333	
160.00	30.13393	3.40565	
150.00	40.58441	3.70338	
140.00	52.52101	3.96121	
130.00	59.52381	4.08638	
120.00	68.68132	4.22948	
110.00	74.40476	4.30952	
100.00	81.16883	4.39653	
90.00	89.28571	4.49184	

TABLE 5

Angle	Sigmatheta	Logsigtheta	Sample
18			23
179.00	121.50221	4.79993	
178.00	75.81803	4.32834	
177.00	59.15863	4.08022	
176.00	46.16132	3.83214	
175.00	29.76190	3.39323	
174.00	18.63354	2.92496	
173.00	15.71428	2.75457	
172.00	15.78073	2.75879	
171.00	16.19047	2.78442	
170.00	18.14059	2.89815	
160.00	29.01785	3.36791	
150.00	40.58441	3.70338	
140.00	52.52101	3.96121	
130.00	58.33333	4.06617	
120.00	67.30769	4.20927	
110.00	71.42857	4.26870	
100.00	81.16883	4.39653	
90.00	89.28571	4.49184	
18			24
179.00	865.24300	6.76301	
178.00	678.37190	6.51970	
177.00	372.48028	5.92018	
176.00	160.34985	5.07736	
175.00	70.34632	4.25343	
174.00	34.16149	3.53110	
173.00	18.92857	2.94067	
172.00	17.02658	2.83478	
171.00	18.57143	2.92162	
170.00	19.27437	2.95878	
160.00	19.01785	2.94538	
150.00	40.58441	3.70338	
140.00	52.52101	3.96121	
130.00	59.52381	4.08638	
120.00	68.68132	4.22948	
110.00	74.40476	4.30952	
100.00	81.16883	4.39653	
90.00	89.28571	4.49184	

TABLE 5

Angle	Sigmatheta	Logsigtheta	Sample
18			25
179.00	77.31959	4.34795	
178.00	57.86113	4.05805	
177.00	56.96757	4.04248	
176.00	38.87269	3.66029	
175.00	27.05627	3.29792	
174.00	19.56521	2.97375	
173.00	16.42857	2.79902	
172.00	15.78073	2.75879	
171.00	16.66666	2.81341	
170.00	18.70748	2.92892	
160.00	30.13393	3.40565	
150.00	42.20779	3.74260	
140.00	54.62185	4.00043	
130.00	61.90476	4.12560	
120.00	71.42857	4.26870	
110.00	77.38095	4.34874	
100.00	84.41558	4.43575	
90.00	92.85714	4.53106	
18			26
179.00	184.09425	5.21545	
178.00	155.62649	5.04746	
177.00	127.08150	4.84483	
176.00	97.18173	4.57658	
175.00	67.64069	4.21421	
174.00	34.16149	3.53110	
173.00	20.71428	3.03082	
172.00	7.48848	2.01337	
171.00	7.50682	2.01581	
170.00	6.79228	1.91579	
160.00	7.84632	2.06004	
150.00	6.73302	1.90702	
140.00	7.02075	1.94887	
130.00	7.14285	1.96611	
120.00	7.26928	1.98366	
110.00	7.49362	2.01405	
100.00	7.40025	2.00151	
90.00	7.46753	2.01056	

TABLE 5

Angle	Sigmatheta	Logsigtheta	Sample
18			27
179.00	38.65979	3.65480	
178.00	25.93774	3.25570	
177.00	12.48904	2.52485	
176.00	8.50340	2.14047	
175.00	4.32900	1.46534	
174.00	2.23602	.80470	
173.00	1.60714	.47446	
172.00	1.49501	.40214	
171.00	1.61904	.48184	
170.00	1.75737	.56382	
160.00	2.79018	1.02611	
150.00	3.89610	1.35998	
140.00	4.83193	1.57525	
130.00	5.47619	1.70041	
120.00	6.59340	1.88607	
110.00	6.84523	1.92355	
100.00	7.46753	2.01056	
90.00	8.57142	2.14843	
18			28
179.00	143.59352	4.96699	
178.00	109.73663	4.69808	
177.00	59.21560	4.08119	
176.00	70.30675	4.25287	
175.00	37.87879	3.63439	
174.00	19.25466	2.95775	
173.00	14.64285	2.68395	
172.00	14.95016	2.70472	
171.00	14.76190	2.69205	
170.00	17.00680	2.83361	
160.00	27.90178	3.32869	
150.00	38.96104	3.66256	
140.00	50.42017	3.92039	
130.00	57.14285	4.04555	
120.00	65.93406	4.18866	
110.00	71.42857	4.26870	
100.00	77.92208	4.35571	
90.00	85.71428	4.45102	

TABLE 5

Angle	Sigmatheta	Logsigtheta	Sample
18			29
179.00	110.45655	4.70462	
178.00	81.80365	4.40432	
177.00	89.83345	4.49796	
176.00	65.59765	4.18354	
175.00	47.46755	3.86005	
174.00	18.94410	2.94149	
173.00	14.64285	2.68395	
172.00	14.11960	2.64756	
171.00	15.23805	2.72380	
170.00	17.00680	2.83361	
160.00	26.78570	3.28787	
150.00	37.33765	3.62000	
140.00	48.31935	3.87783	
130.00	54.76190	4.00299	
120.00	63.18680	4.14610	
110.00	66.96430	4.20416	
100.00	74.67530	4.31315	
90.00	82.14285	4.40846	
18			30
179.00	607.51104	6.40937	
178.00	438.94653	6.08438	
177.00	262.92725	5.57188	
176.00	116.61807	4.75890	
175.00	51.40692	3.93977	
174.00	22.67080	3.12108	
173.00	16.07143	2.77704	
172.00	15.36545	2.73212	
171.00	15.23809	2.72380	
170.00	16.43991	2.79971	
160.00	25.11160	3.22333	
150.00	35.71428	3.57555	
140.00	45.16806	3.81039	
130.00	52.38095	3.95854	
120.00	60.43956	4.10164	
110.00	65.47619	4.18169	
100.00	71.42857	4.26870	
90.00	78.57143	4.36401	

TABLE 5

Angle	Sigmatheta	Logsigtheta	Sample
18			31
179.00	114.13844	4.73741	
178.00	81.80367	4.40432	
177.00	65.73181	4.18558	
176.00	51.02041	3.93223	
175.00	29.76190	3.39323	
174.00	17.39130	2.85597	
173.00	12.85714	2.55390	
172.00	13.28903	2.58694	
171.00	14.76190	2.69205	
170.00	16.43991	2.79971	
160.00	27.90178	3.32869	
150.00	40.58441	3.70338	
140.00	52.52101	3.96121	
130.00	57.14285	4.04555	
120.00	65.93406	4.18866	
110.00	71.42857	4.26870	
100.00	77.92208	4.35571	
90.00	85.71428	4.45102	
18			32
179.00	533.33333	6.27915	
178.00	69.27374	4.23807	
177.00	58.89570	4.07577	
176.00	35.13513	3.55920	
175.00	22.12121	3.09654	
174.00	16.69565	2.81515	
173.00	14.80000	2.69463	
172.00	12.55813	2.53037	
171.00	11.73333	2.46243	
170.00	10.79365	2.37896	
160.00	13.75000	2.62104	
150.00	20.00000	2.99573	
140.00	25.88200	3.25355	
130.00	28.00000	3.33220	
120.00	32.30769	3.47531	
110.00	27.33333	3.30811	
100.00	29.45454	3.38285	
90.00	29.45454	3.38285	

TABLE 5

Angle	Sigmatheta	Logsigtheta	Sample
18			33
179.00	984.61538	6.89225	
178.00	102.79329	4.63272	
177.00	61.34969	4.11659	
176.00	43.24324	3.76684	
175.00	23.93939	3.17553	
174.00	17.39130	2.85597	
173.00	13.20000	2.58022	
172.00	11.62790	2.45341	
171.00	10.66666	2.36712	
170.00	10.79365	2.37896	
160.00	15.00000	2.70805	
150.00	13.18181	2.57884	
140.00	18.82352	2.93511	
130.00	21.60000	3.07269	
120.00	25.23076	3.22806	
110.00	27.00000	3.29584	
100.00	29.09090	3.37043	
90.00	31.27272	3.44275	
18			34
179.00	574.35897	6.35325	
178.00	53.63128	3.98213	
177.00	44.17177	3.78809	
176.00	10.13513	2.31601	
175.00	18.18181	2.90042	
174.00	13.21739	2.58153	
173.00	10.79999	2.37955	
172.00	9.76744	2.27905	
171.00	9.06666	2.20460	
170.00	9.52380	2.25379	
160.00	12.50000	2.52573	
150.00	14.72727	2.68970	
140.00	19.05882	2.94753	
130.00	21.60000	3.07269	
120.00	24.92307	3.21579	
110.00	27.00000	3.29584	
100.00	28.72727	3.35785	
90.00	29.09090	3.37043	

TABLE 5

Angle	Sigmatheta	Logsigtheta	Sample
18			35
179.00	861.53846	6.75872	
178.00	71.50837	4.26981	
177.00	49.07975	3.89345	
176.00	35.13513	3.55920	
175.00	19.39393	2.96496	
174.00	15.65217	2.75061	
173.00	14.40000	2.66723	
172.00	13.02325	2.56674	
171.00	9.60000	2.26176	
170.00	10.15873	2.31833	
160.00	10.75000	2.37491	
150.00	15.09090	2.71409	
140.00	19.05882	2.94753	
130.00	21.33333	3.06027	
120.00	25.23076	3.22806	
110.00	27.33333	3.30811	
100.00	29.81818	3.39512	
90.00	29.45454	3.38285	
18			36
179.00	779.48717	6.65864	
178.00	71.50837	4.26981	
177.00	46.62576	3.84215	
176.00	37.83783	3.63331	
175.00	22.42424	3.11014	
174.00	14.95652	2.70515	
173.00	12.00000	2.48491	
172.00	10.69767	2.37003	
171.00	9.60000	2.26176	
170.00	10.15873	2.31833	
160.00	10.75000	2.37491	
150.00	14.90909	2.70197	
140.00	19.29411	2.95980	
130.00	21.60000	3.07269	
120.00	24.30769	3.19079	
110.00	27.00000	3.29584	
100.00	29.45454	3.38285	
90.00	29.45454	3.38285	

TABLE 5

Angle	Sigmatheta	Logsigtheta	Sample
	18		37
179.00	1194.23076	7.08526	
178.00	151.95530	5.02359	
177.00	107.97546	4.68190	
176.00	83.78378	4.42824	
175.00	60.60606	4.10439	
174.00	45.21739	3.81148	
173.00	31.19999	3.44042	
172.00	26.04651	3.25988	
171.00	24.00000	3.17805	
170.00	23.49456	3.15677	
160.00	16.25000	2.78809	
150.00	18.18181	2.90042	
140.00	19.29411	2.95980	
130.00	21.33333	3.06027	
120.00	24.61538	3.20337	
110.00	26.33333	3.27084	
100.00	28.36363	3.34511	
90.00	29.09090	3.37043	
	18		38
179.00	1169.23077	7.06410	
178.00	105.02793	4.65423	
177.00	51.53374	3.94224	
176.00	37.83784	3.63331	
175.00	24.84848	3.21280	
174.00	16.34782	2.79409	
173.00	12.40000	2.51770	
172.00	10.69767	2.37003	
171.00	10.13333	2.31583	
170.00	10.15873	2.31833	
160.00	10.87500	2.38647	
150.00	14.54545	2.67728	
140.00	19.05882	2.94753	
130.00	21.33333	3.06027	
120.00	24.61538	3.20337	
110.00	26.66666	3.28341	
100.00	29.09091	3.37043	
90.00	29.45454	3.38285	

TABLE 5

Angle	Sigmatheta	Logsigtheta	Sample
	18		39
179.00	1374.35897	7.22574	
178.00	71.50838	4.26981	
177.00	58.89570	4.07577	
176.00	37.83784	3.63331	
175.00	22.72727	3.12357	
174.00	17.04348	2.83577	
173.00	14.00000	2.63906	
172.00	11.62790	2.45341	
171.00	11.20000	2.41591	
170.00	11.42857	2.43612	
160.00	10.75000	2.37491	
150.00	15.27272	2.72607	
140.00	19.52941	2.97192	
130.00	21.86666	3.08496	
120.00	25.53846	3.24019	
110.00	27.33333	3.30811	
100.00	29.81818	3.39512	
90.00	29.81818	3.39512	
	18		40
179.00	1600.00000	7.37776	
178.00	160.89385	5.08074	
177.00	56.44172	4.03321	
176.00	45.94594	3.82747	
175.00	23.03030	3.13681	
174.00	17.04348	2.83577	
173.00	14.40000	2.66723	
172.00	12.09302	2.49263	
171.00	11.20000	2.41591	
170.00	11.42857	2.43612	
160.00	15.00000	2.70805	
150.00	15.45454	2.73790	
140.00	19.52941	2.97192	
130.00	22.40000	3.10906	
120.00	25.53846	3.24019	
110.00	27.66666	3.32023	
100.00	30.54545	3.41922	
90.00	29.81818	3.39512	

TABLE 5

Angle	Sigmatheta	Logsigtheta	Sample
	18		41
179.00	1579.48718	7.36486	
178.00	158.65922	5.06676	
177.00	56.44172	4.03321	
176.00	43.24324	3.76684	
175.00	23.93939	3.17553	
174.00	18.78261	2.93293	
173.00	14.80000	2.69463	
172.00	13.48837	2.60183	
171.00	12.80000	2.54945	
170.00	12.69841	2.54148	
160.00	15.00000	2.70805	
150.00	15.09091	2.71409	
140.00	19.52941	2.97192	
130.00	22.13333	3.09708	
120.00	25.53846	3.24019	
110.00	27.66666	3.32023	
100.00	30.18182	3.40724	
90.00	29.81818	3.39512	
	18		42
179.00	1025.64102	6.93307	
178.00	122.90502	4.81141	
177.00	61.34969	4.11659	
176.00	40.54054	3.70230	
175.00	24.24242	3.18810	
174.00	28.52173	3.35067	
173.00	23.59999	3.16125	
172.00	20.00000	2.99573	
171.00	17.60000	2.86790	
170.00	16.50793	2.80384	
160.00	25.00000	3.21888	
150.00	21.81818	3.08274	
140.00	19.76470	2.98390	
130.00	22.40000	3.10906	
120.00	25.53846	3.24019	
110.00	27.33333	3.30811	
100.00	29.81818	3.39512	
90.00	29.81818	3.39512	

TABLE 5

Angle	Sigmatheta	Logsigtheta	Sample
18			43
179.00	6.97435	1.94224	
178.00	7.59776	2.02785	
177.00	8.09815	2.09164	
176.00	8.64864	2.15740	
175.00	9.69696	2.27181	
174.00	11.13043	2.40968	
173.00	12.40000	2.51770	
172.00	13.95348	2.63573	
171.00	15.46666	2.73869	
170.00	17.77777	2.87795	
160.00	26.25000	3.26767	
150.00	30.90909	3.43105	
140.00	35.29411	3.56372	
130.00	34.66666	3.54578	
120.00	36.92307	3.60884	
110.00	40.00000	3.68888	
100.00	33.09090	3.49926	
90.00	32.00000	3.46574	
18			44
179.00	615.38461	6.42225	
178.00	491.62011	6.19771	
177.00	392.63803	5.97289	
176.00	351.35135	5.86179	
175.00	230.30303	5.43940	
174.00	222.60869	5.40542	
173.00	204.00000	5.31812	
172.00	190.69767	5.25069	
171.00	181.33333	5.20034	
170.00	177.77777	5.18053	
160.00	71.25000	4.26619	
150.00	49.09090	3.89367	
140.00	42.35294	3.74604	
130.00	40.00000	3.68888	
120.00	40.00000	3.68888	
110.00	40.00000	3.68888	
100.00	34.18181	3.53169	
90.00	33.81818	3.52100	

TABLE 5

Angle	Sigmatheta	Logsigtheta	Sample
18			45
179.00	84.68336	4.43892	
178.00	57.86113	4.05805	
177.00	54.77651	4.00326	
176.00	46.16132	3.83214	
175.00	35.17316	3.56028	
174.00	22.98136	3.13468	
173.00	20.00000	2.99573	
172.00	19.51827	2.97135	
171.00	20.00000	2.99573	
170.00	21.54195	3.07000	
160.00	30.13393	3.40565	
150.00	12.72015	2.54319	
140.00	52.52101	3.96121	
130.00	59.52381	4.08638	
120.00	68.68132	4.22948	
110.00	74.40476	4.30952	
100.00	81.16883	4.39653	
90.00	89.28571	4.49184	
18			46
179.00	239.32253	5.47781	
178.00	87.78780	4.47492	
177.00	61.34969	4.11659	
176.00	46.16132	3.83214	
175.00	32.46753	3.48024	
174.00	22.04969	3.09330	
173.00	18.92857	2.94067	
172.00	18.68770	2.92787	
171.00	17.61905	2.86898	
170.00	18.70748	2.92892	
160.00	30.13393	3.40565	
150.00	40.58441	3.70338	
140.00	52.52101	3.96121	
130.00	61.90476	4.12560	
120.00	71.42857	4.26870	
110.00	77.38095	4.34874	
100.00	87.66234	4.47349	
90.00	92.85714	4.53106	

APPENDIX II

ILLUSTRATIONS

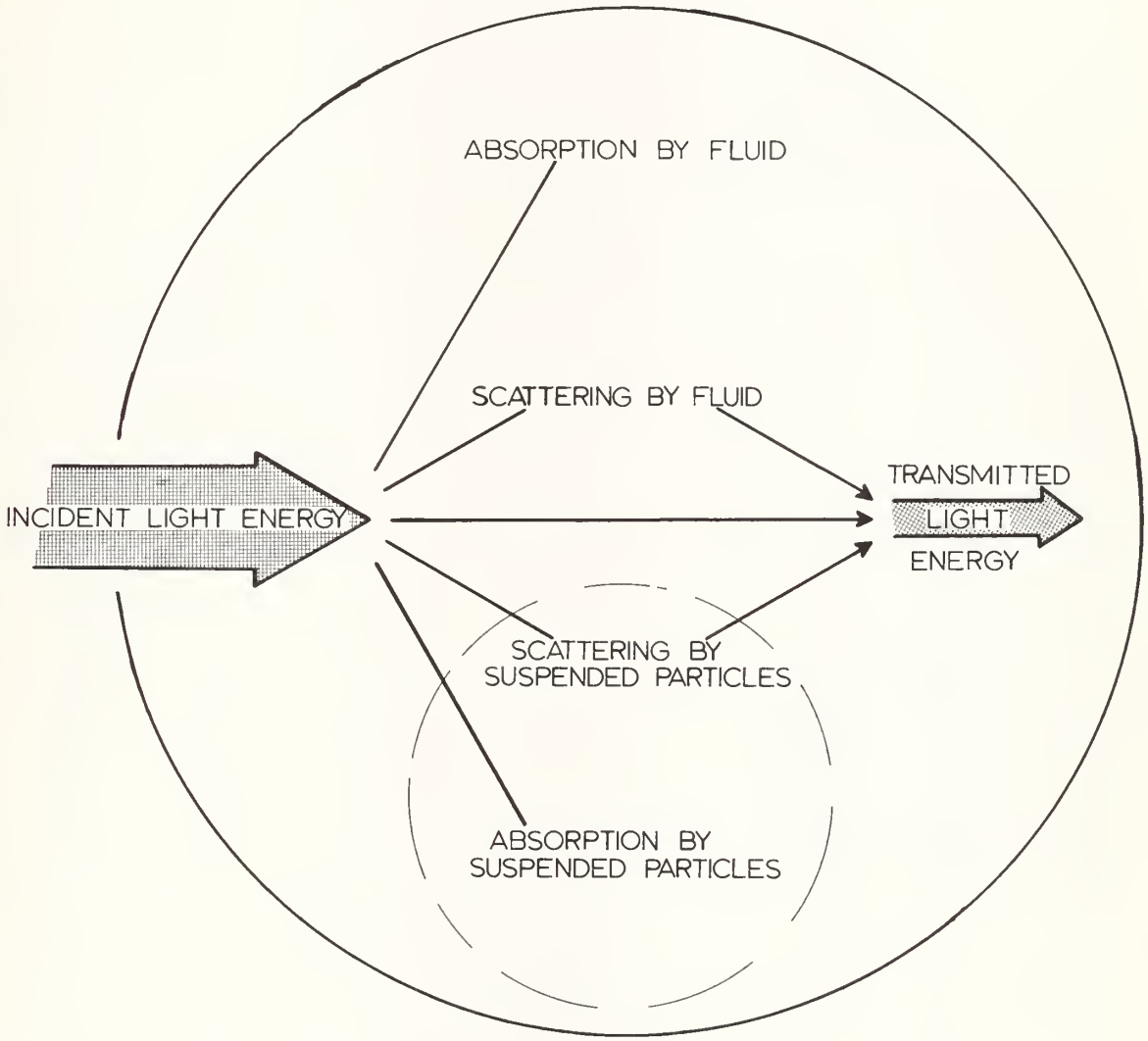

LIGHT ENERGY ATTENUATION

FIGURE 1

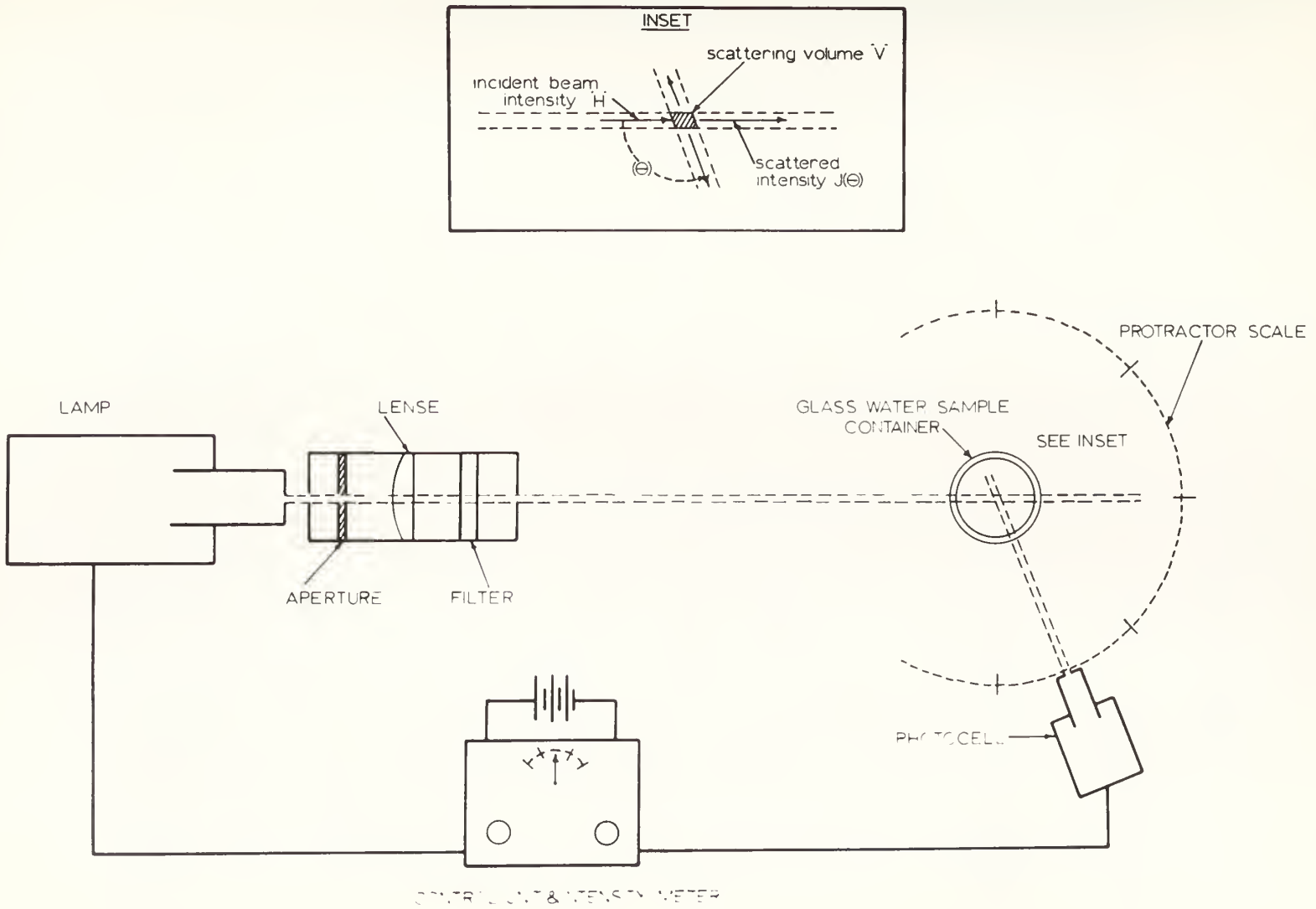

SCHEMATIC SCATTERCMETER

FIGURE 2

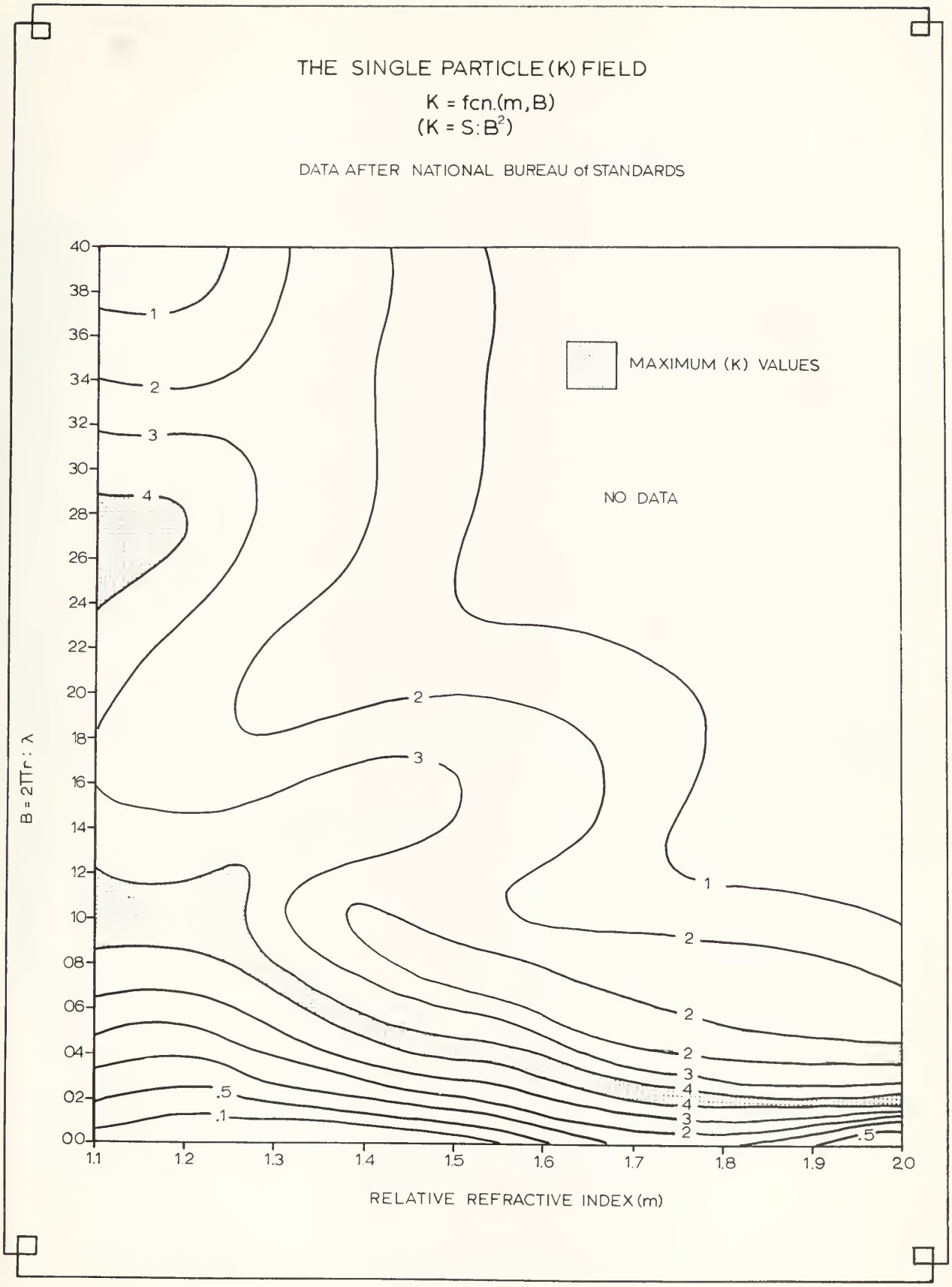
THE SINGLE PARTICLE (K) FIELD
K = fcn.(m, B)
(K = S:B²)
DATA AFTER NATIONAL BUREAU of STANDARDS
MAXIMUM (K) VALUES
NO DATA
B = 2Tr : λ
RELATIVE REFRACTIVE INDEX (m)
40
38
36
34
32
30
28
26
24
22
20
18
16
14
12
10
08
06
04
02
00
1.1
1.2
1.3
1.4
1.5
1.6
1.7
1.8
1.9
2.0
1
2
3
4
.5
.1

FIGURE 3

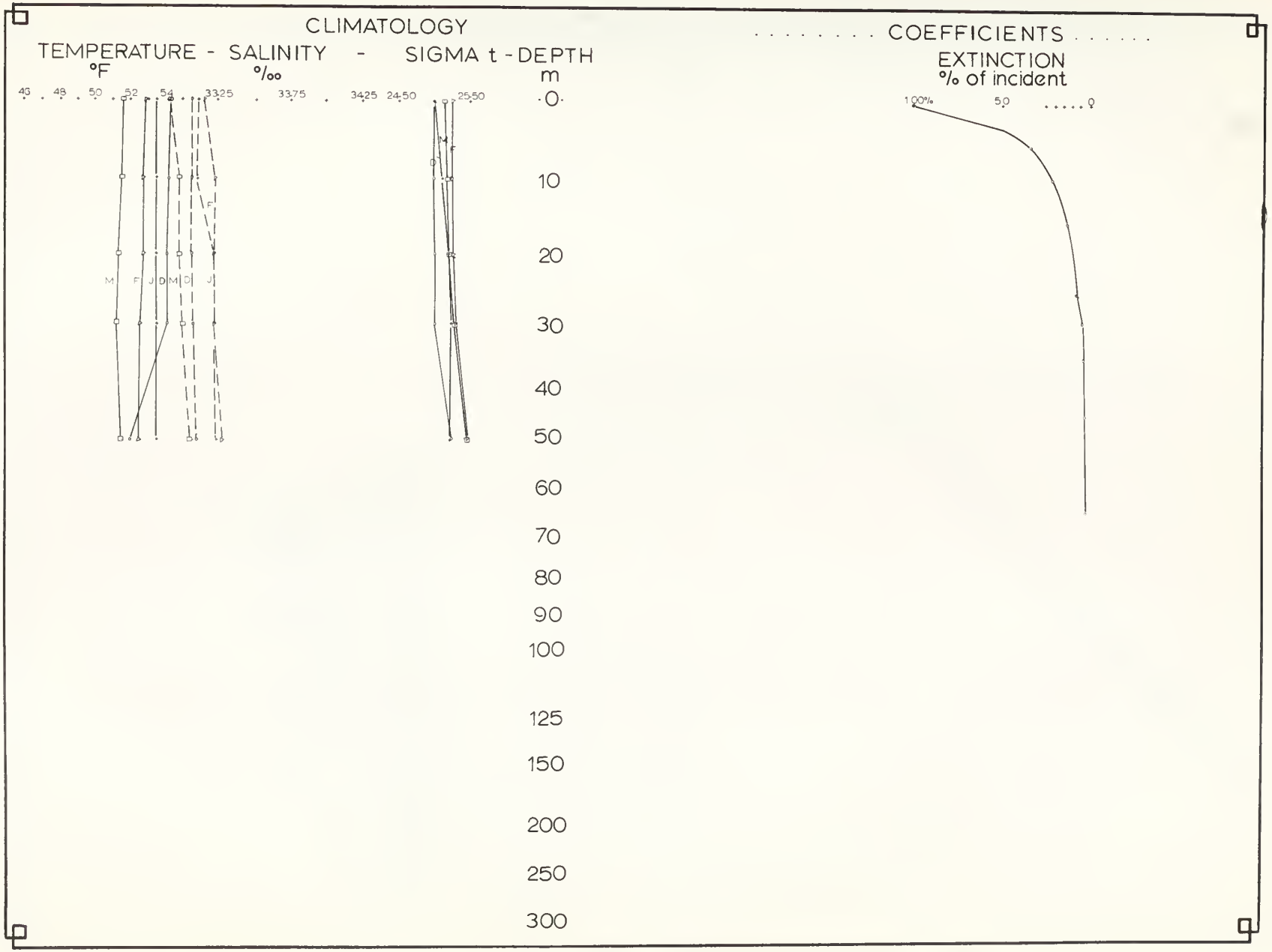
CLIMATOLOGY
TEMPERATURE - SALINITY - SIGMA t - DEPTH
°F
‰
m
43 48 50 52 54 33.25 33.75 34.25 24.50 25.50
0
10
20
30
40
50
60
70
80
90
100
125
150
200
250
300
M F J D M D J
COEFFICIENTS
EXTINCTION
% of incident
100% 50 0

FIGURE 4

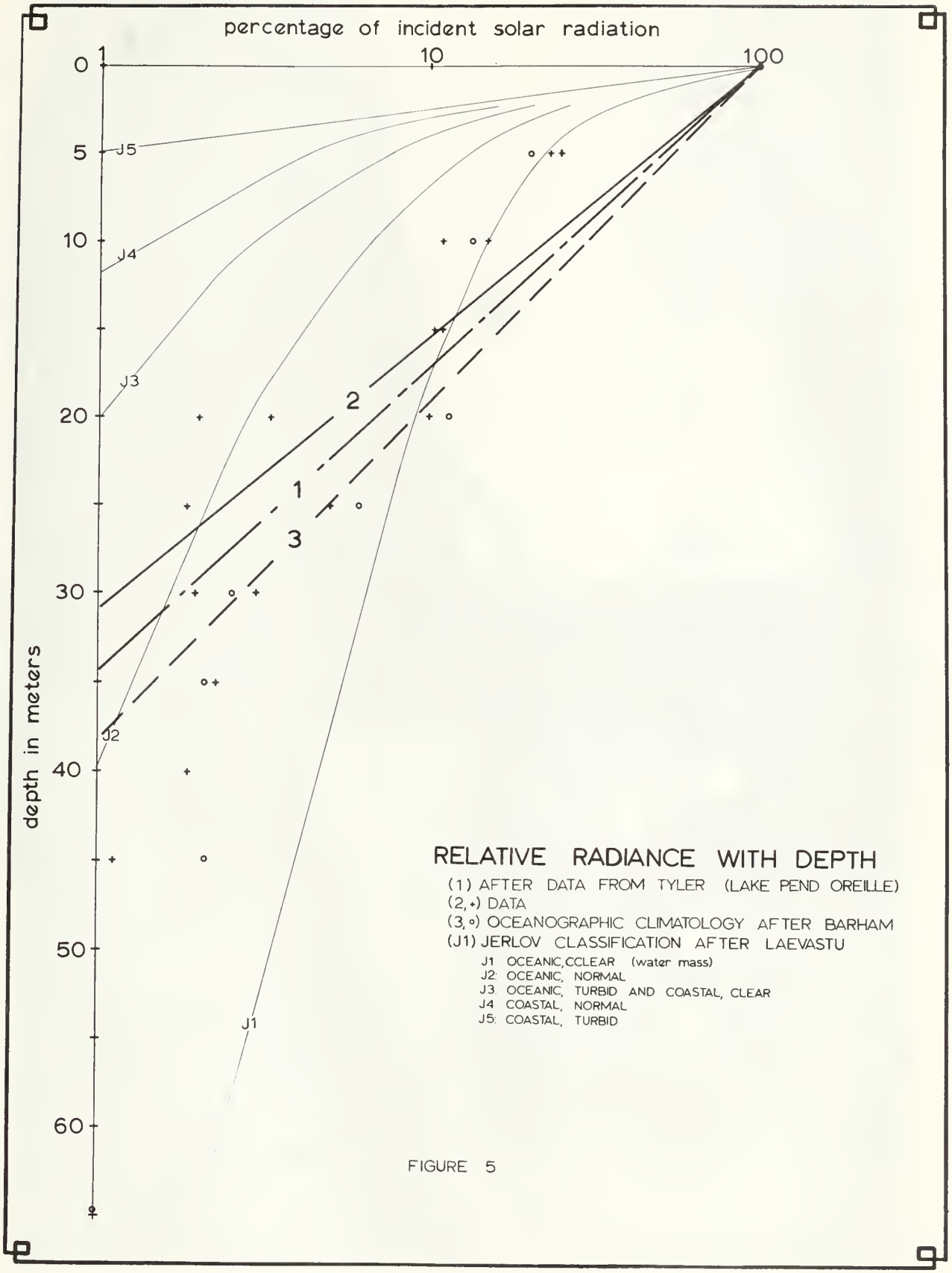

RELATIVE RADIANCE WITH DEPTH

(1) AFTER DATA FROM TYLER (LAKE PEND OREILLE)
(2, +) DATA
(3, ∘) OCEANOGRAPHIC CLIMATOLOGY AFTER BARHAM
(J1) JERLOV CLASSIFICATION AFTER LAEVASTU

- J1 OCEANIC, CCLEAR (water mass)
- J2 OCEANIC, NORMAL
- J3 OCEANIC, TURBID AND COASTAL, CLEAR
- J4 COASTAL, NORMAL
- J5 COASTAL, TURBID

FIGURE 5

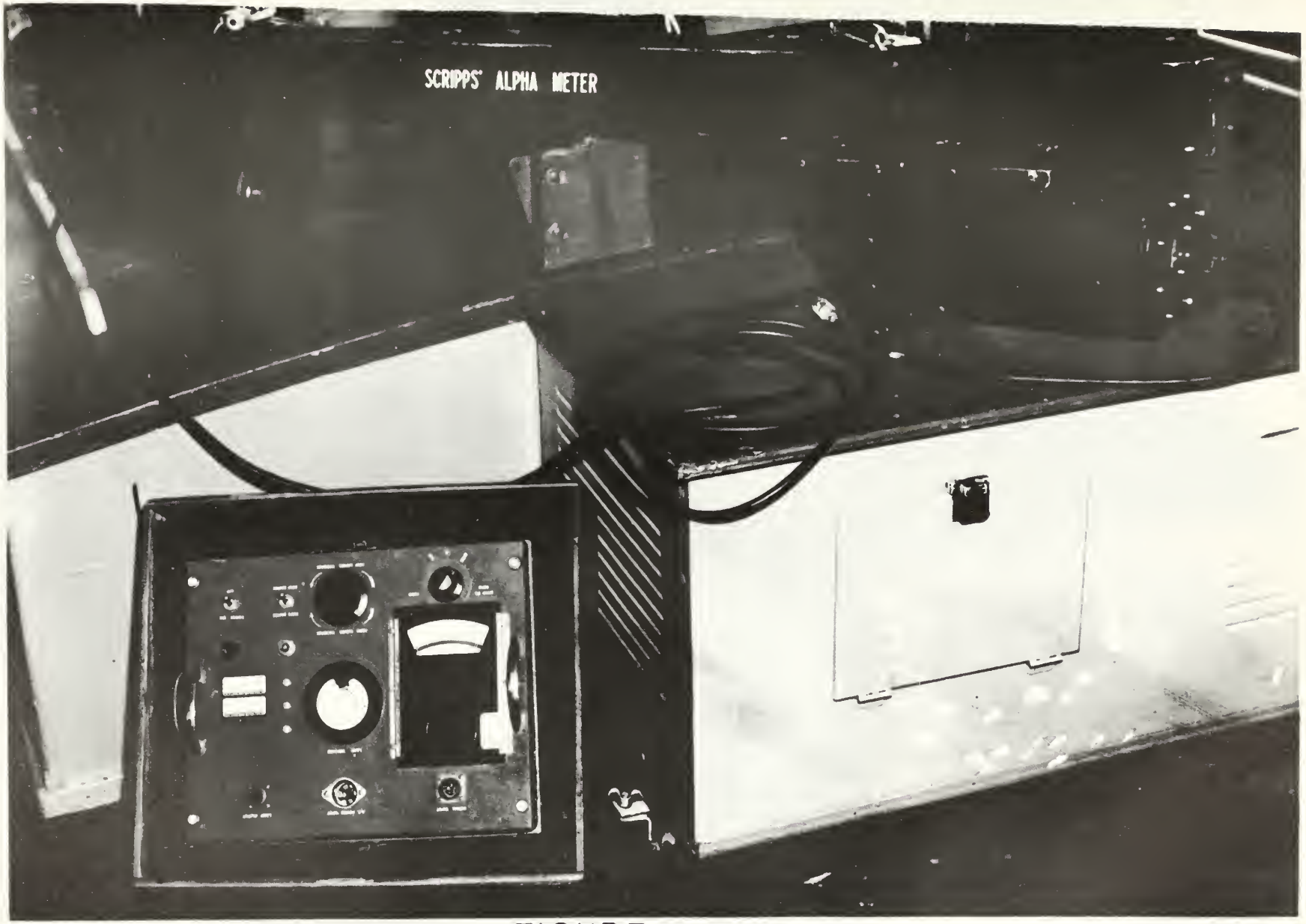

FIGURE 6

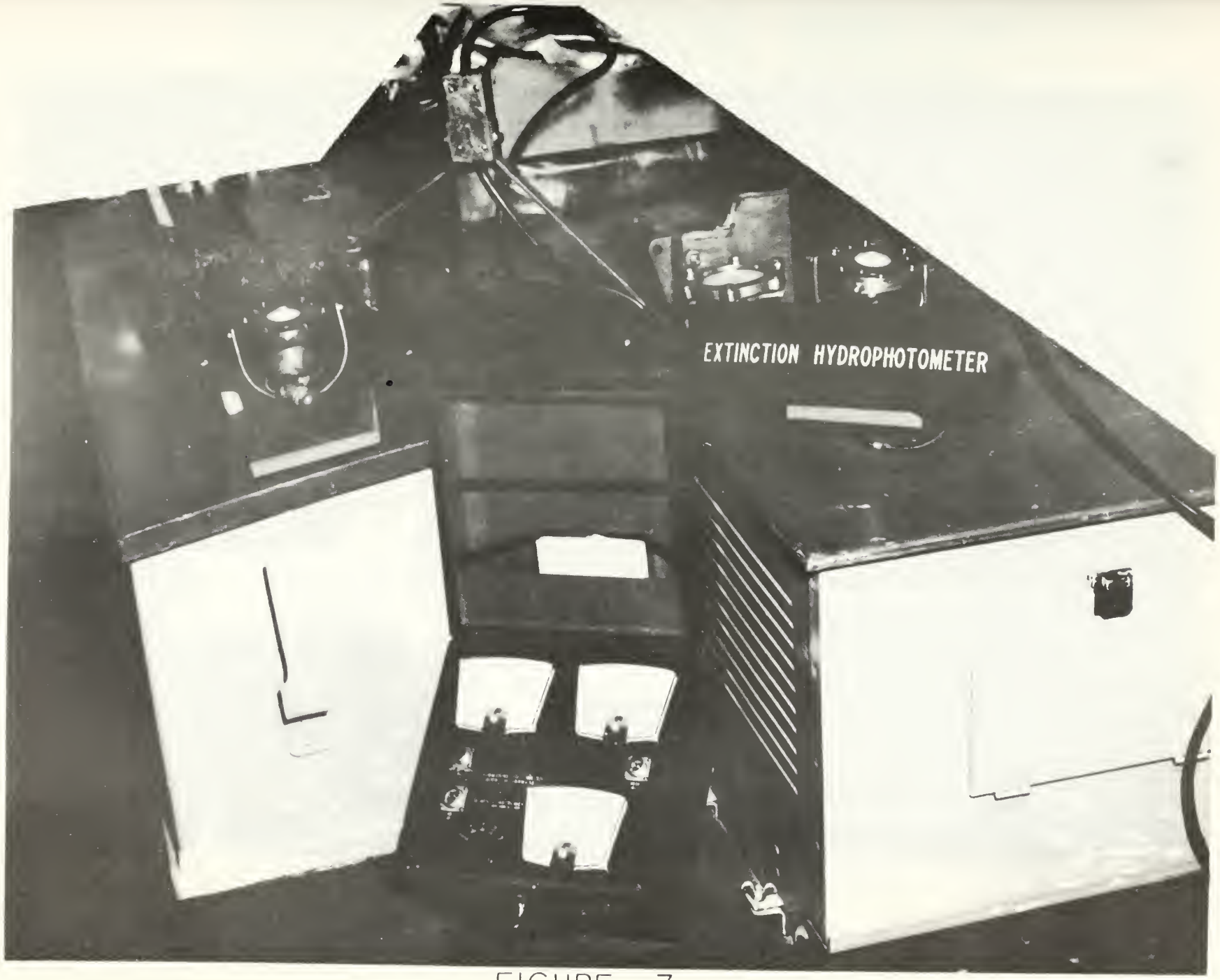

FIGURE 7

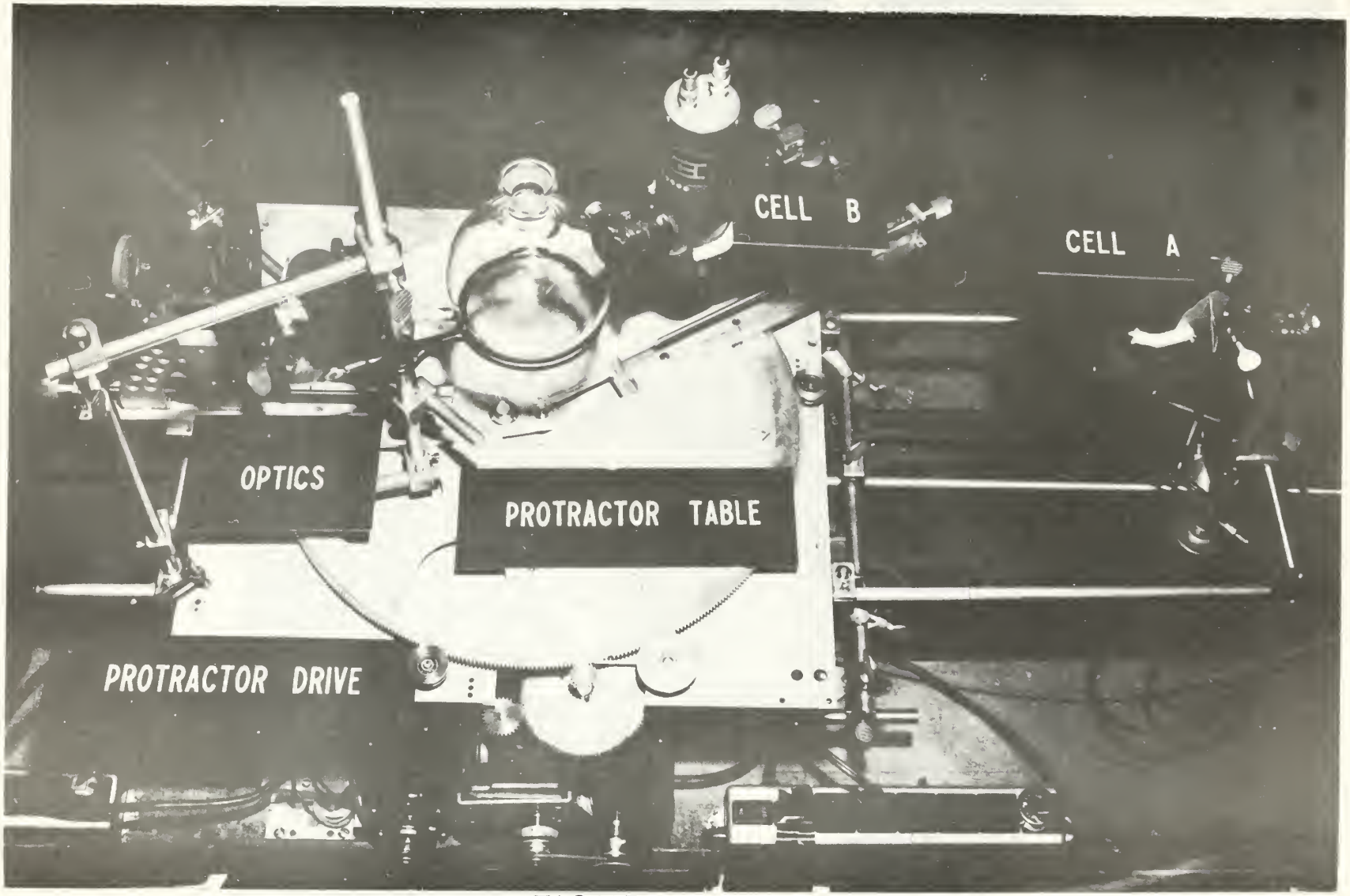

FIGURE 8


XENON ARC LAMP
OPTICS
CELL B
CELL A
PROTRACTOR TABLE
PROTRACTOR DRIVE
DIFFERENTIAL PHOTOMETER

FIGURE 9

FIGURE 10

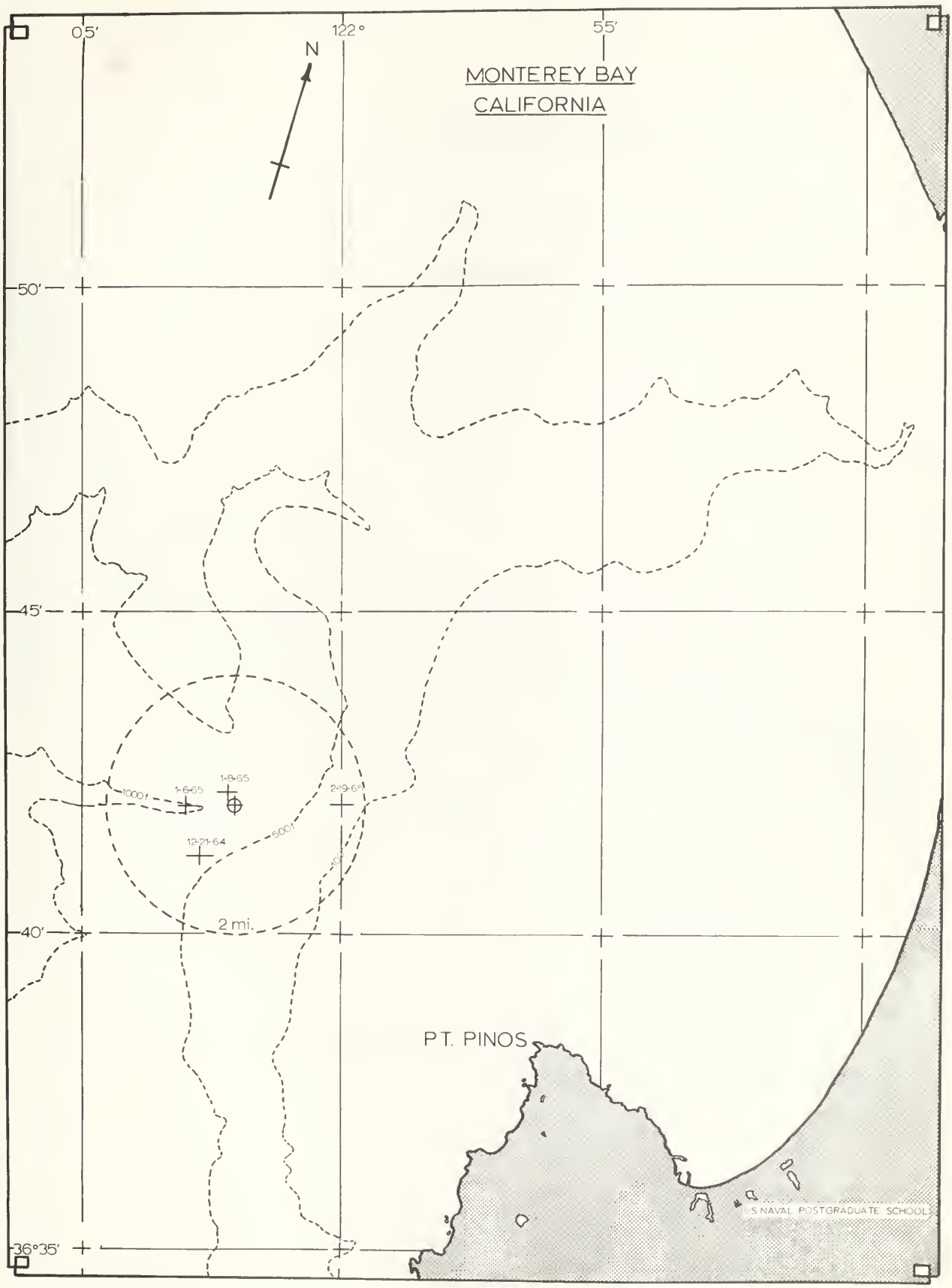
05'
122°
55'
N
MONTEREY BAY
CALIFORNIA
50'
45'
40'
36°35'
1000'
1-6-65
1-8-65
2-19-65
12-21-64
500'
2 mi.
PT. PINOS
S NAVAL POSTGRADUATE SCHOOL

FIGURE 11

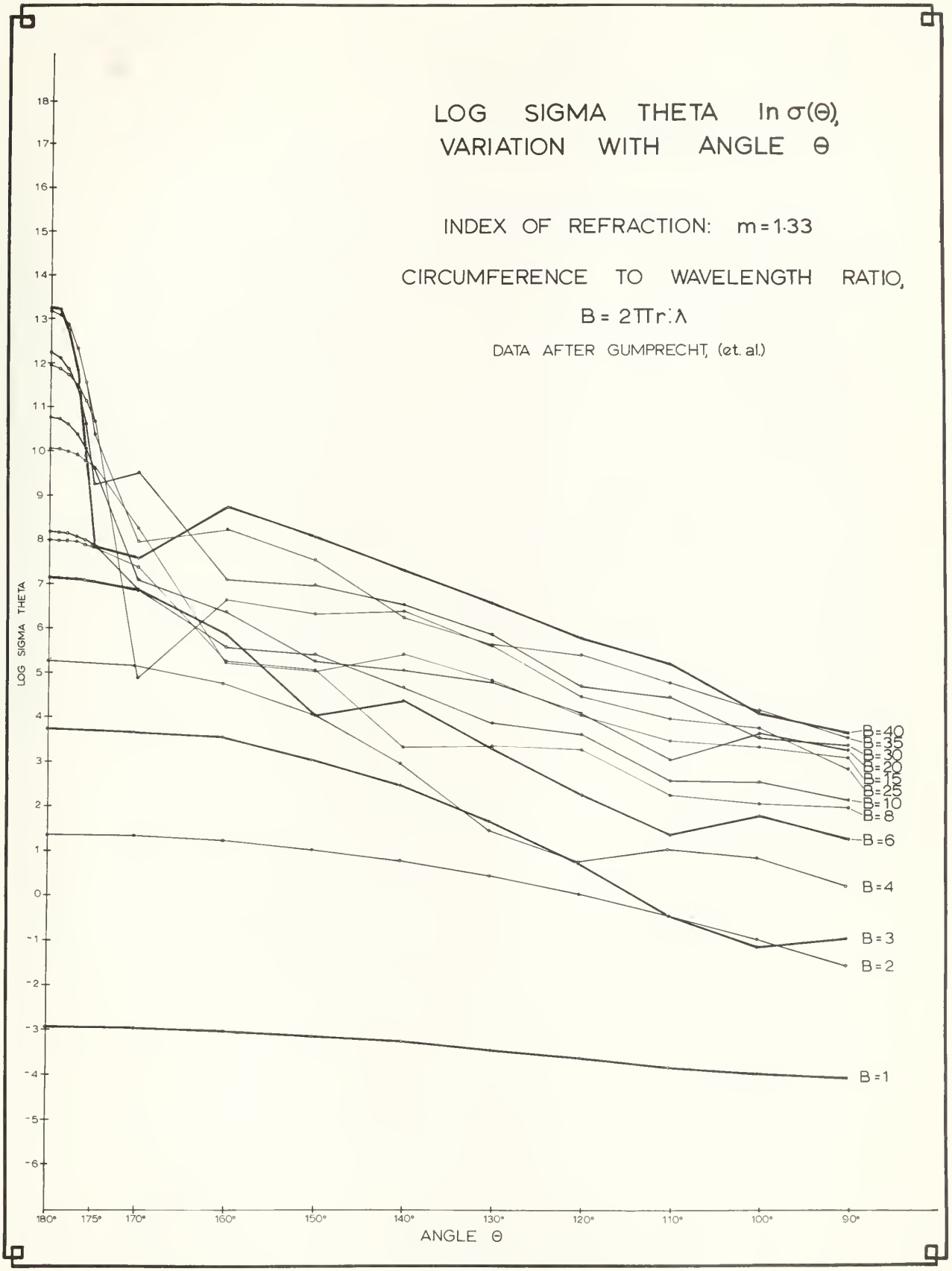
LOG SIGMA THETA ln σ(Θ),
VARIATION WITH ANGLE Θ
INDEX OF REFRACTION: m = 1·33
CIRCUMFERENCE TO WAVELENGTH RATIO,
B = 2πr ÷ λ
DATA AFTER GUMPRECHT, (et. al.)
LOG SIGMA THETA
ANGLE Θ
B=40
B=35
B=30
B=25
B=20
B=15
B=10
B=8
B=6
B=4
B=3
B=2
B=1

FIGURE 12

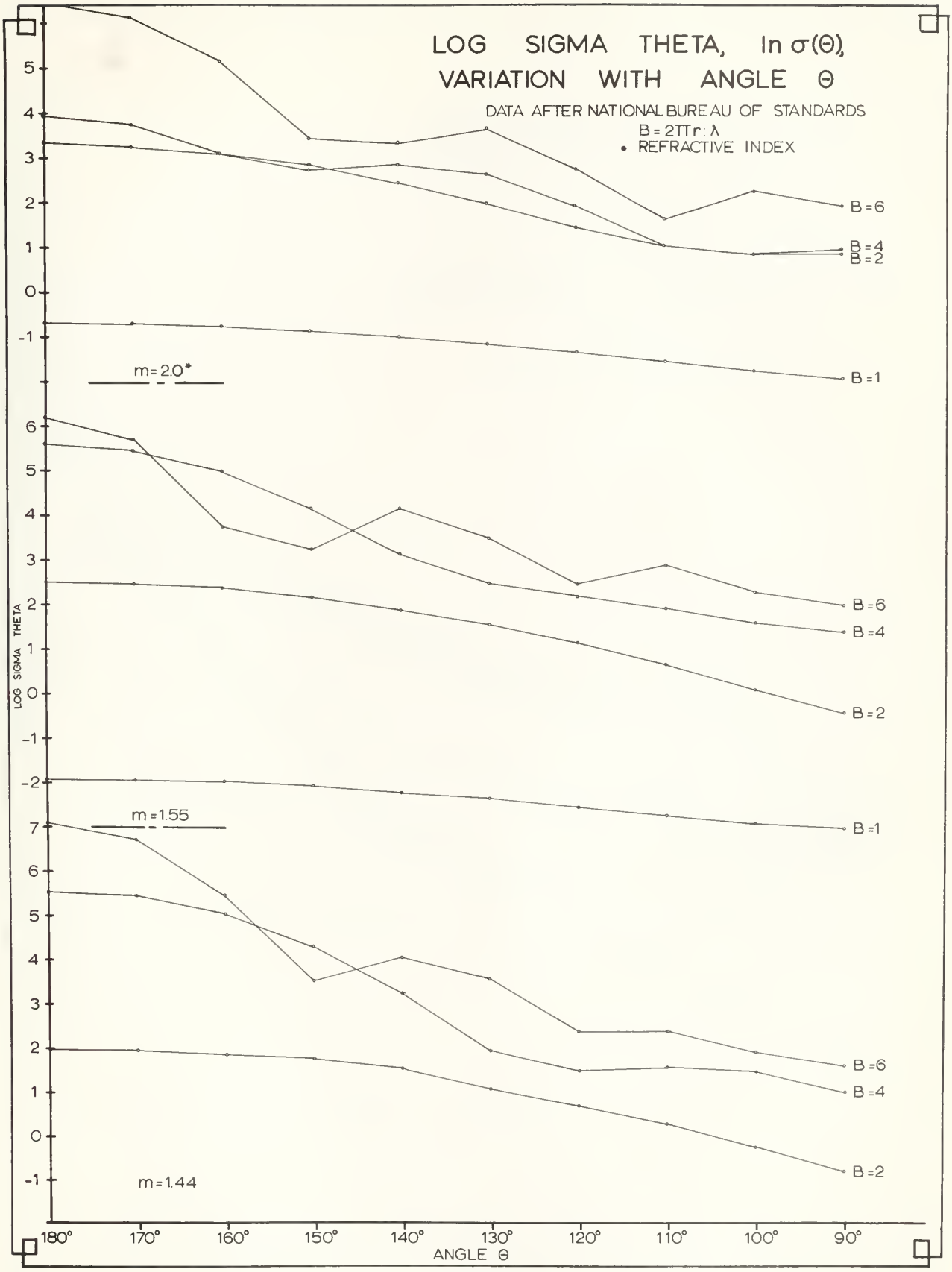
LOG SIGMA THETA, ln σ(Θ),
VARIATION WITH ANGLE Θ
DATA AFTER NATIONAL BUREAU OF STANDARDS
B = 2πr : λ
• REFRACTIVE INDEX
B = 6
B = 4
B = 2
B = 1
m = 2.0*
B = 6
B = 4
B = 2
B = 1
m = 1.55
B = 6
B = 4
B = 2
m = 1.44
LOG SIGMA THETA
180° 170° 160° 150° 140° 130° 120° 110° 100° 90°
ANGLE Θ

FIGURE 13

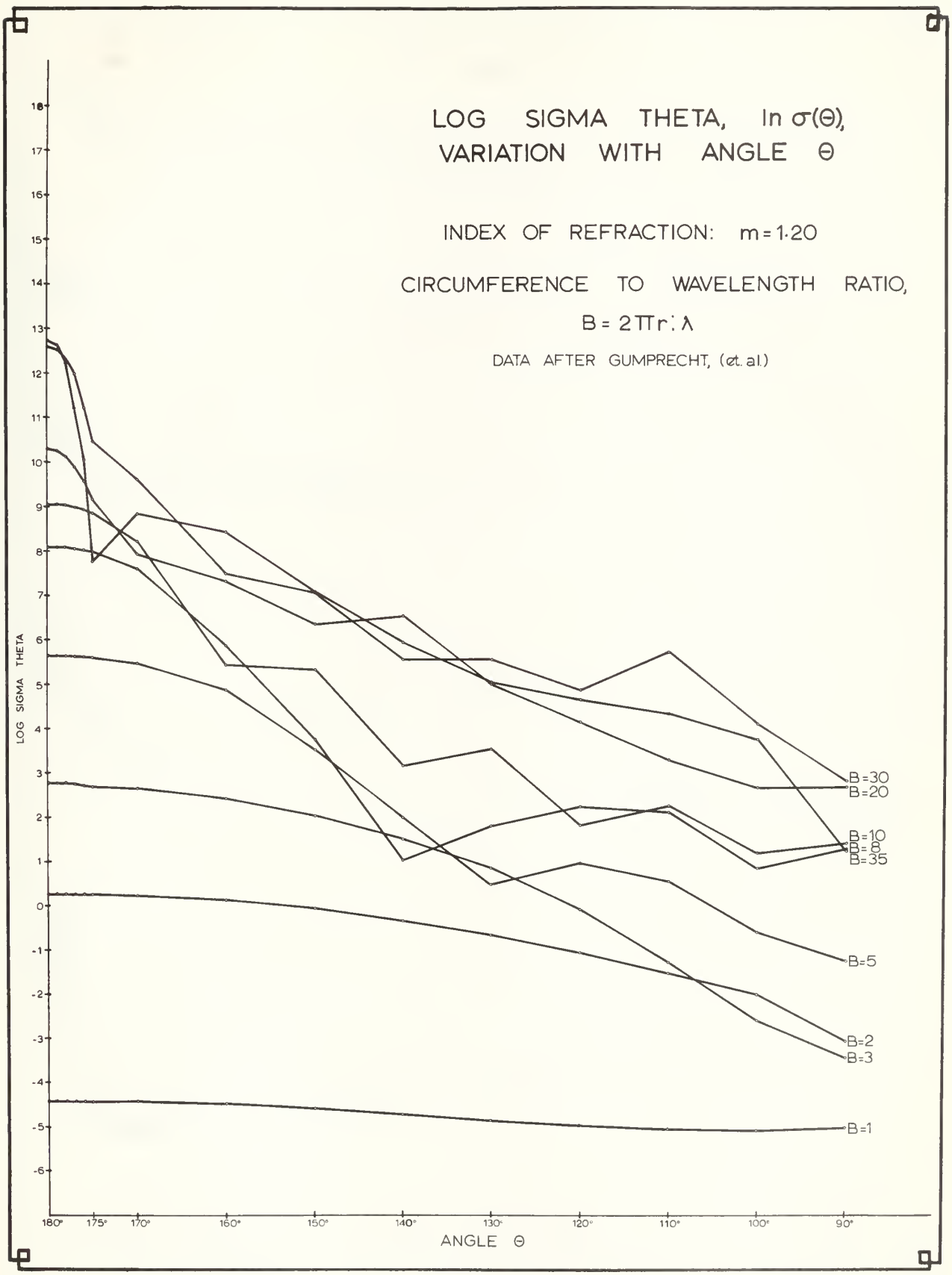
LOG SIGMA THETA, ln σ(Θ),
VARIATION WITH ANGLE Θ
INDEX OF REFRACTION: m = 1·20
CIRCUMFERENCE TO WAVELENGTH RATIO,
B = 2πr : λ
DATA AFTER GUMPRECHT, (et. al.)
LOG SIGMA THETA
ANGLE Θ
B=30
B=20
B=10
B=8
B=35
B=5
B=2
B=3
B=1

FIGURE 14

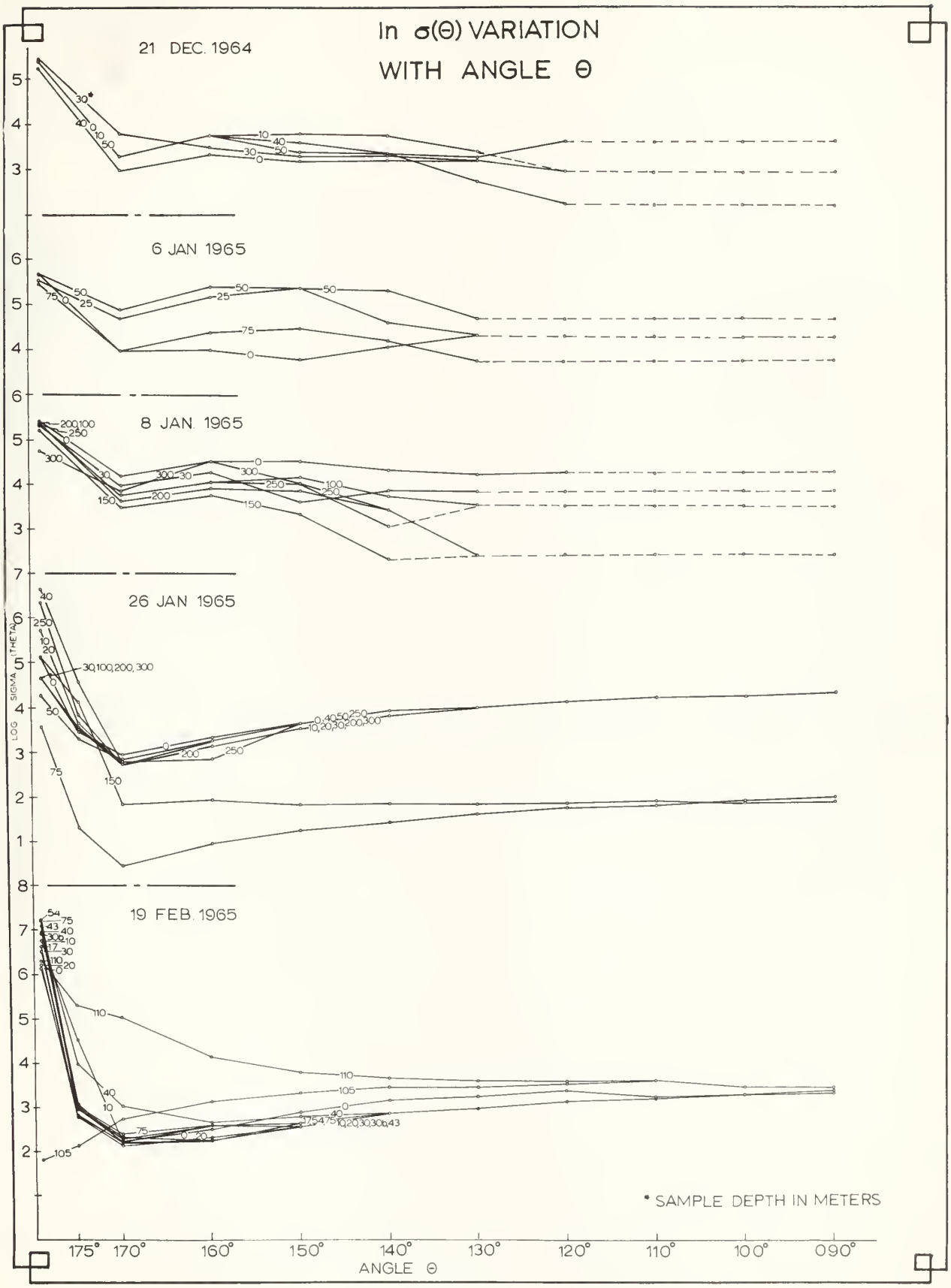
ln σ(Θ) VARIATION
WITH ANGLE Θ
21 DEC. 1964
6 JAN 1965
8 JAN. 1965
26 JAN 1965
19 FEB. 1965
LOG SIGMA (THETA)
* SAMPLE DEPTH IN METERS
175° 170° 160° 150° 140° 130° 120° 110° 100° 090°
ANGLE Θ

FIGURE 15

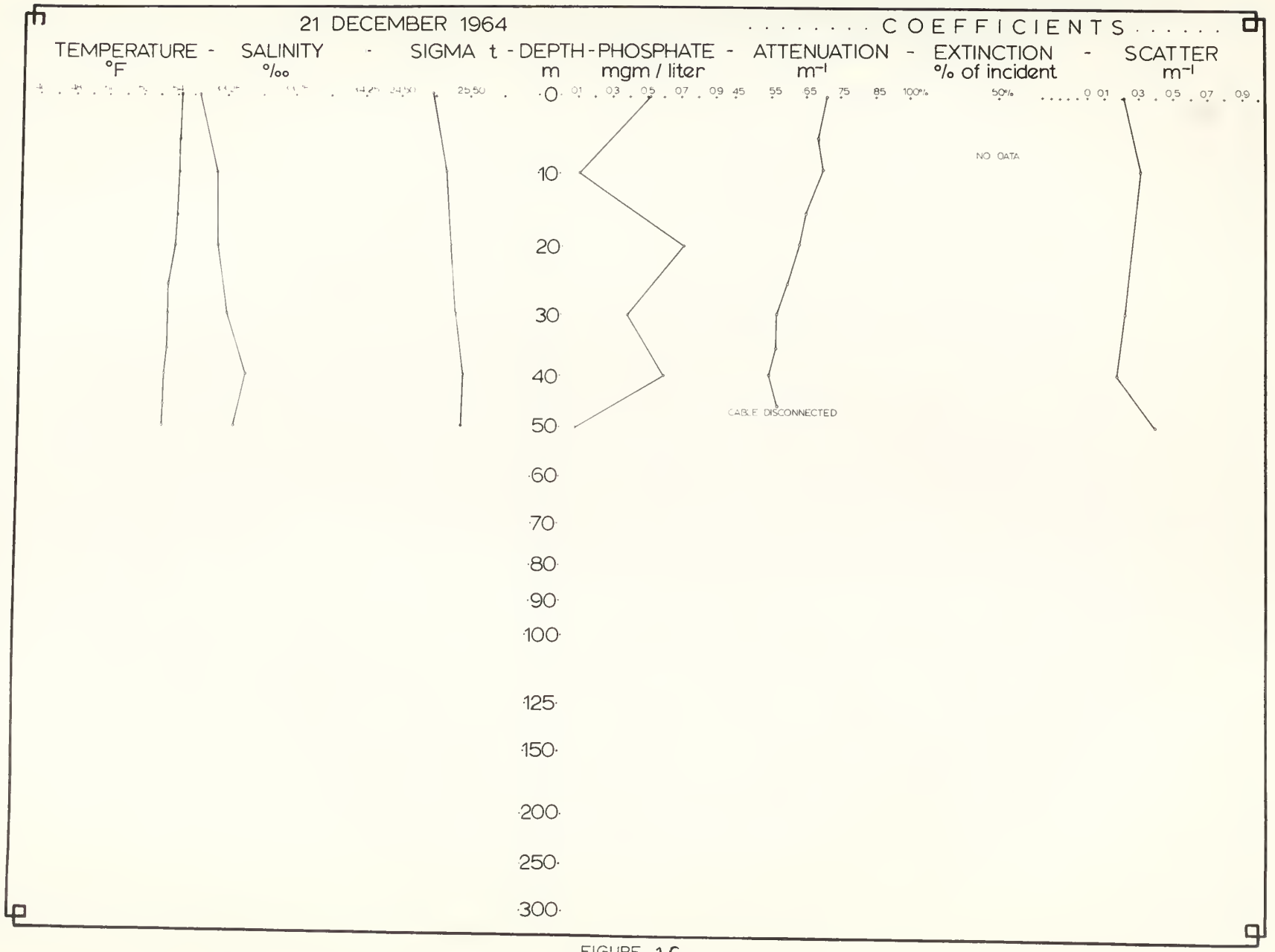
21 DECEMBER 1964
COEFFICIENTS
TEMPERATURE - °F
SALINITY - ‰
SIGMA t
DEPTH - m
PHOSPHATE - mgm / liter
ATTENUATION - m⁻¹
EXTINCTION - % of incident
SCATTER - m⁻¹
0
10
20
30
40
50
60
70
80
90
100
125
150
200
250
300
0.1 0.3 0.5 0.7 0.9
45 55 65 75 85 100%
50%
0 0.1 0.3 0.5 0.7 0.9
NO DATA
CABLE DISCONNECTED

FIGURE 16

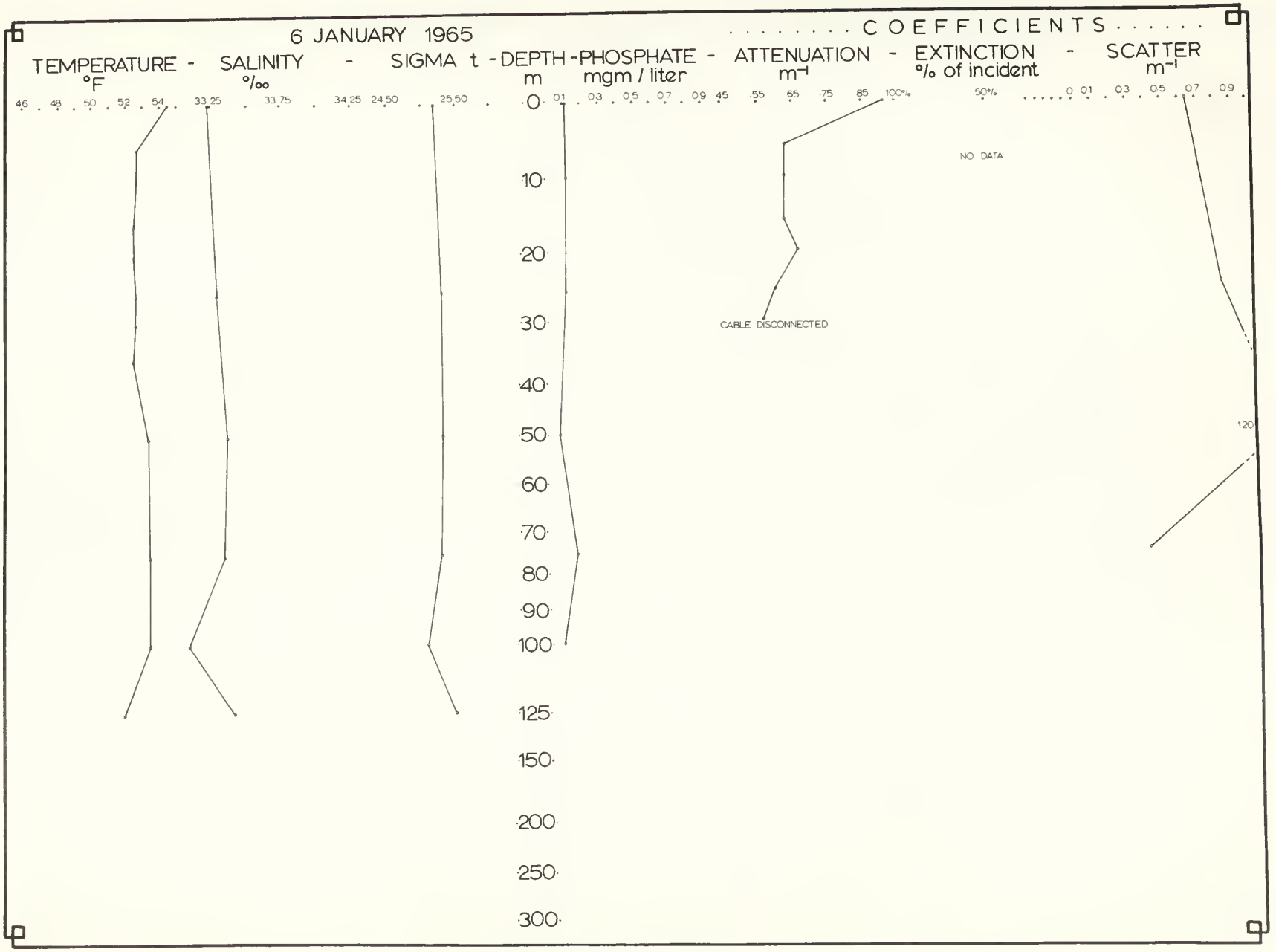
6 JANUARY 1965
COEFFICIENTS
TEMPERATURE °F
SALINITY °/oo
SIGMA t
DEPTH m
PHOSPHATE mgm / liter
ATTENUATION m⁻¹
EXTINCTION % of incident
SCATTER m⁻¹
46 48 50 52 54
33.25 33.75 34.25 24.50 25.50
0 10 20 30 40 50 60 70 80 90 100 125 150 200 250 300
0.1 0.3 0.5 0.7 0.9
45 55 65 75 85 100%
CABLE DISCONNECTED
NO DATA
50%
0 0.1 0.3 0.5 0.7 0.9
120

FIGURE 17

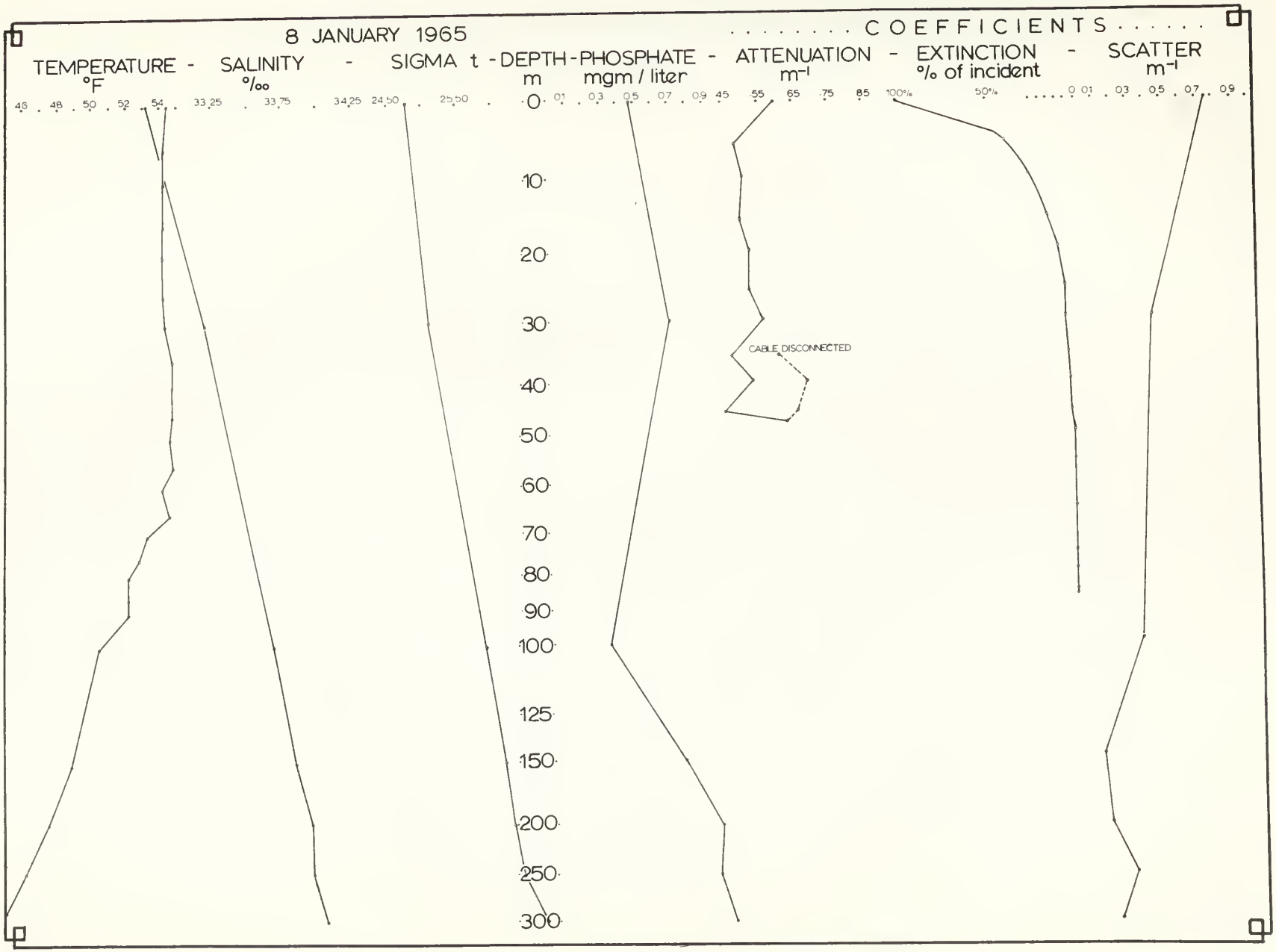
8 JANUARY 1965
COEFFICIENTS
TEMPERATURE - °F
SALINITY - °/oo
SIGMA t
DEPTH - m
PHOSPHATE - mgm / liter
ATTENUATION - m⁻¹
EXTINCTION - % of incident
SCATTER - m⁻¹
46 48 50 52 54
33.25 33.75 34.25
24.50 25.50
0 10 20 30 40 50 60 70 80 90 100 125 150 200 250 300
0 .01 .03 .05 .07 .09
45 55 65 75 85 100%
50%
0 .01 .03 .05 .07 .09
CABLE DISCONNECTED

FIGURE 18

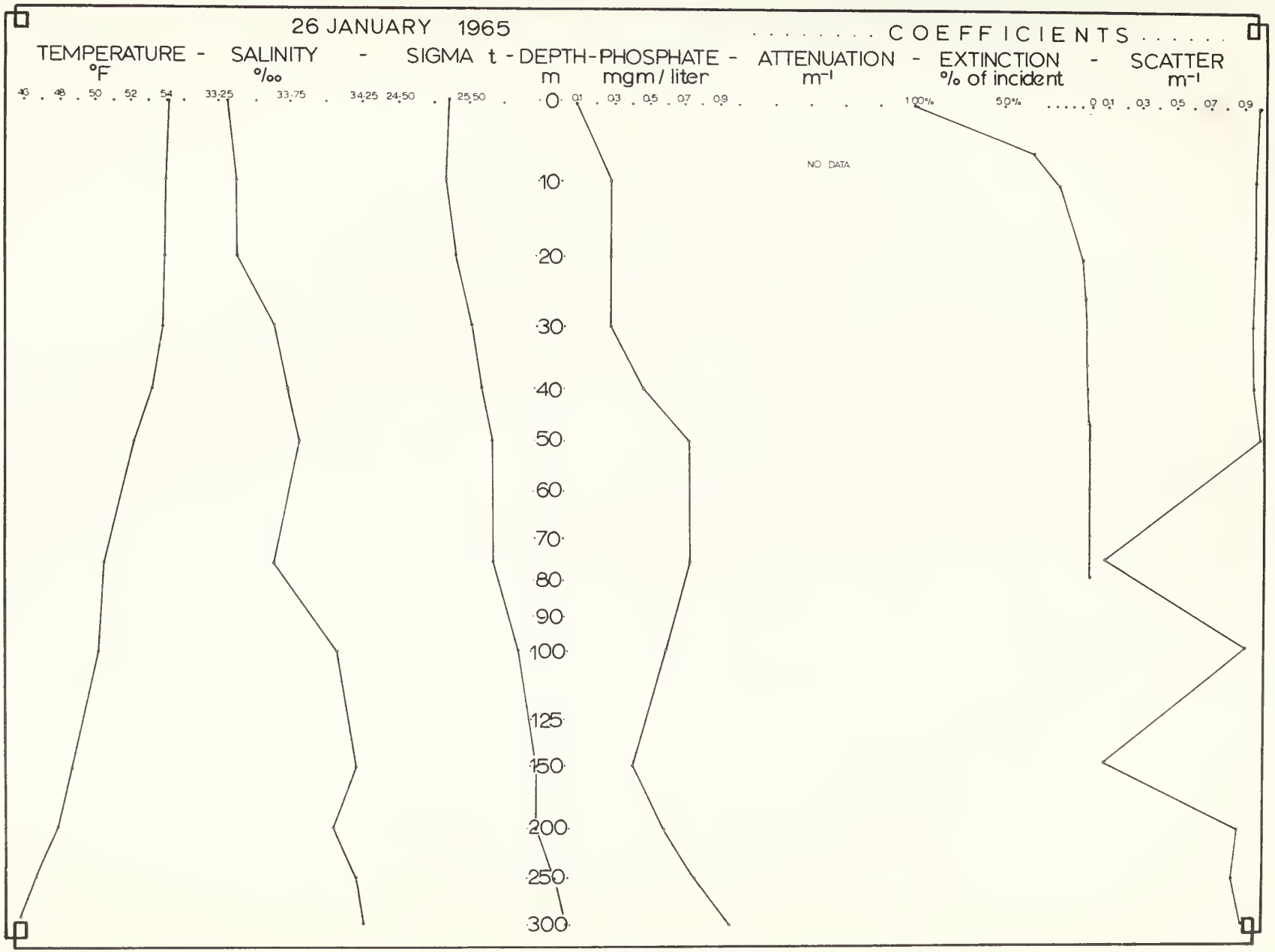
26 JANUARY 1965
COEFFICIENTS
TEMPERATURE - °F
SALINITY - ‰
SIGMA t -
DEPTH - m
PHOSPHATE - mgm / liter
ATTENUATION - m⁻¹
EXTINCTION - % of incident
SCATTER - m⁻¹
46 48 50 52 54
33.25 33.75 34.25
24.50 25.50
0 10 20 30 40 50 60 70 80 90 100 125 150 200 250 300
0.1 0.3 0.5 0.7 0.9
NO DATA
100%
50%
0 0.1 0.3 0.5 0.7 0.9

FIGURE 19

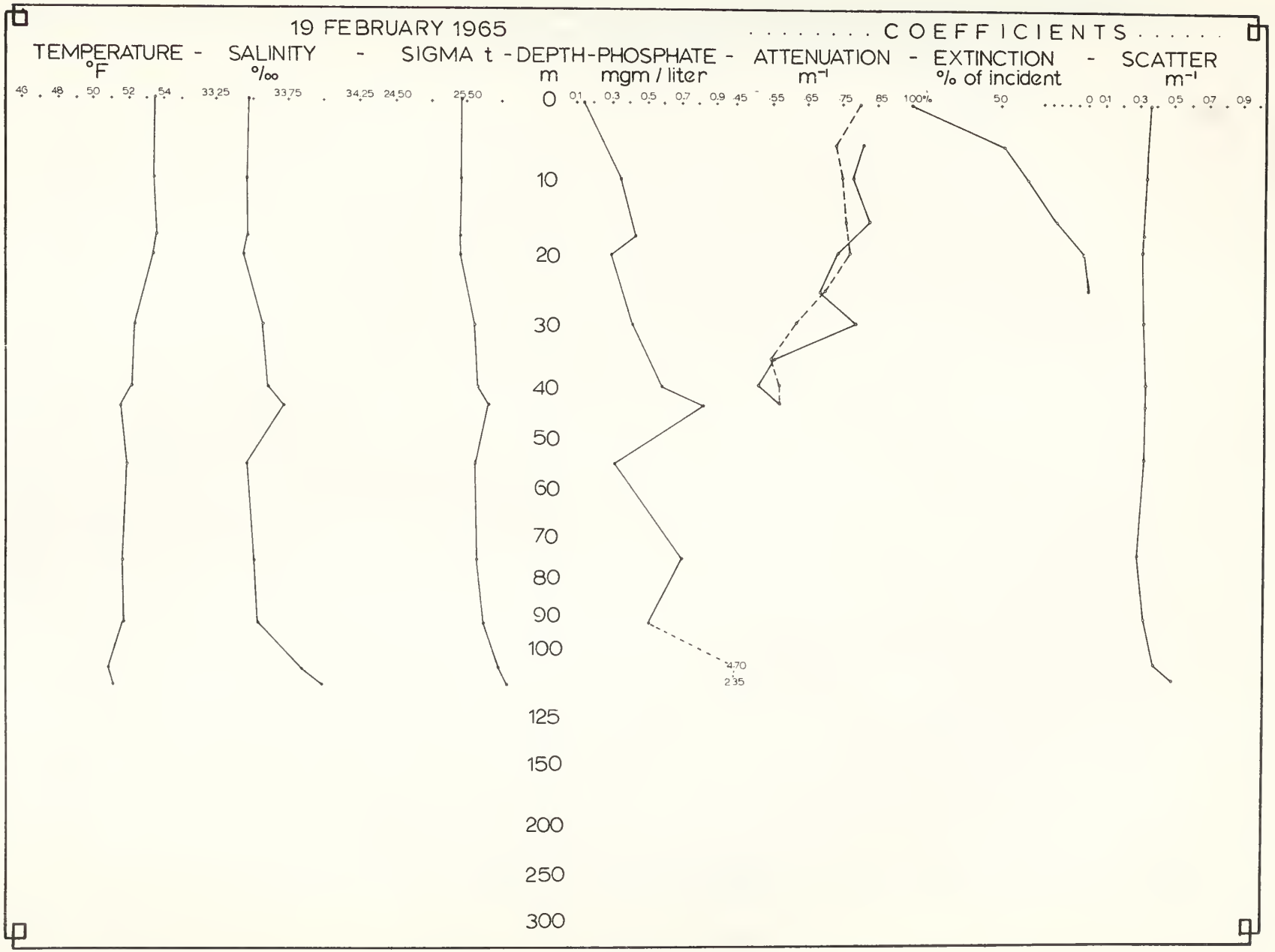
19 FEBRUARY 1965
COEFFICIENTS
TEMPERATURE - °F
SALINITY - ‰
SIGMA t
DEPTH - m
PHOSPHATE - mgm / liter
ATTENUATION - m⁻¹
EXTINCTION - % of incident
SCATTER - m⁻¹
46 48 50 52 54
33.25 33.75
34.25 24.50 25.50
0 10 20 30 40 50 60 70 80 90 100 125 150 200 250 300
0.1 0.3 0.5 0.7 0.9
.45 .55 .65 .75 .85
100%
50
0 0.1 0.3 0.5 0.7 0.9
4.70
2.35

FIGURE 20

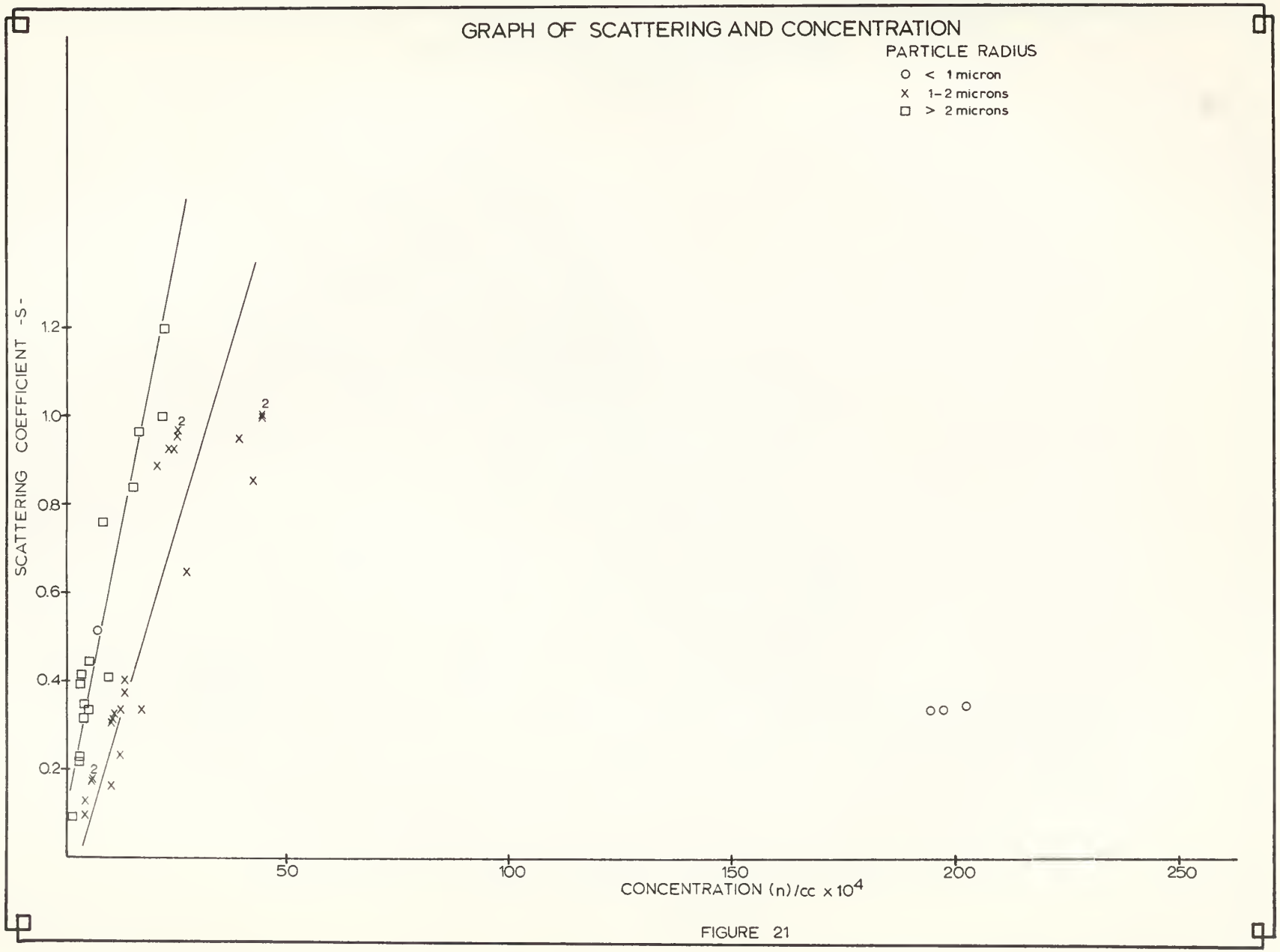
GRAPH OF SCATTERING AND CONCENTRATION
PARTICLE RADIUS
○ < 1 micron
× 1-2 microns
□ > 2 microns
SCATTERING COEFFICIENT -S-
1.2
1.0
0.8
0.6
0.4
0.2
50
100
150
200
250
CONCENTRATION (n)/cc x 10^4

FIGURE 21

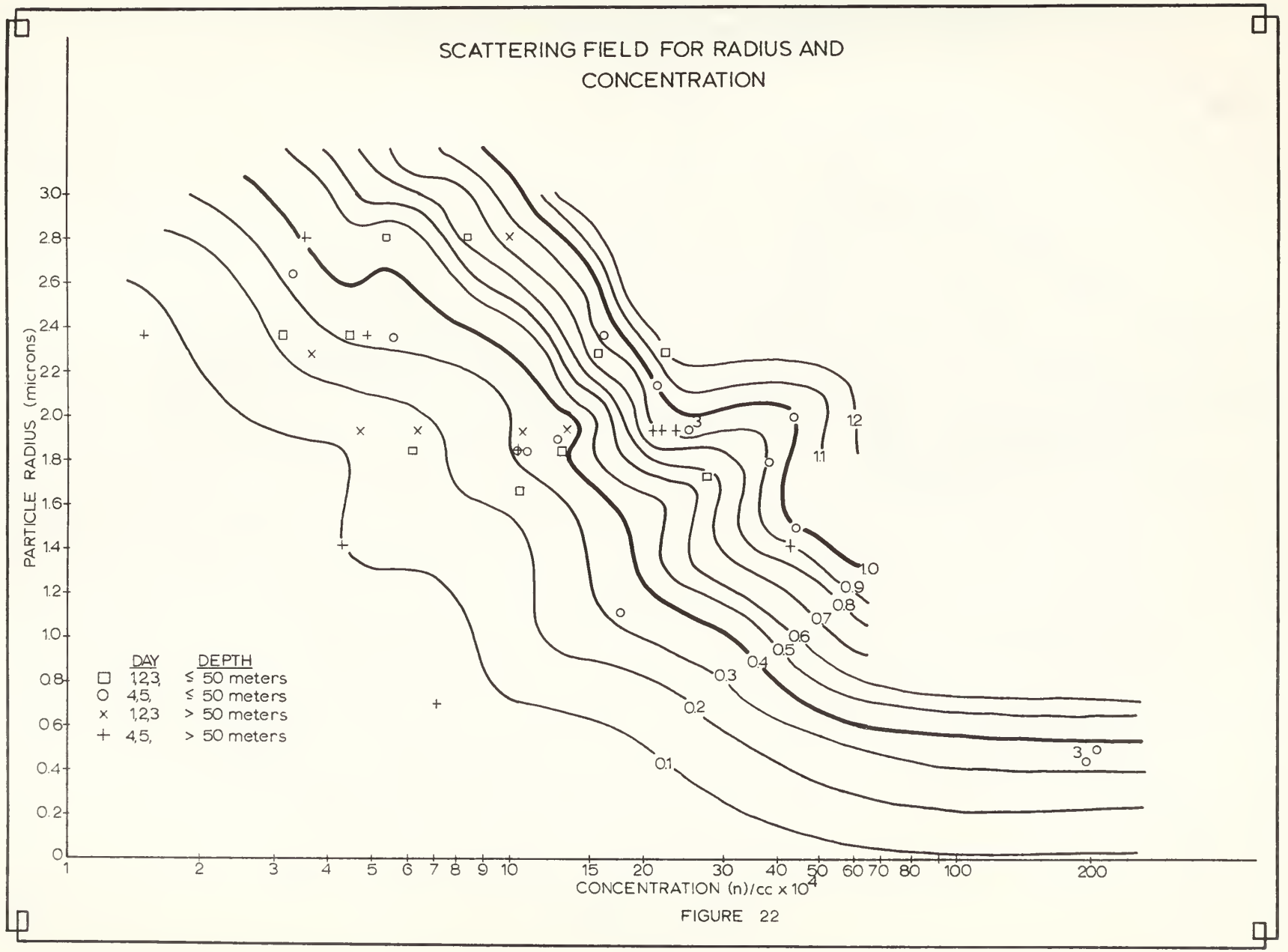
SCATTERING FIELD FOR RADIUS AND CONCENTRATION
PARTICLE RADIUS (microns)
3.0
2.8
2.6
2.4
2.2
2.0
1.8
1.6
1.4
1.2
1.0
0.8
0.6
0.4
0.2
0
DAY DEPTH
□ 1,2,3, ≤ 50 meters
○ 4,5, ≤ 50 meters
× 1,2,3 > 50 meters
+ 4,5, > 50 meters
1.2
1.1
1.0
0.9
0.8
0.7
0.6
0.5
0.4
0.3
0.2
0.1
3
1 2 3 4 5 6 7 8 9 10 15 20 30 40 50 60 70 80 100 200
CONCENTRATION (n)/cc x 10^4

FIGURE 22

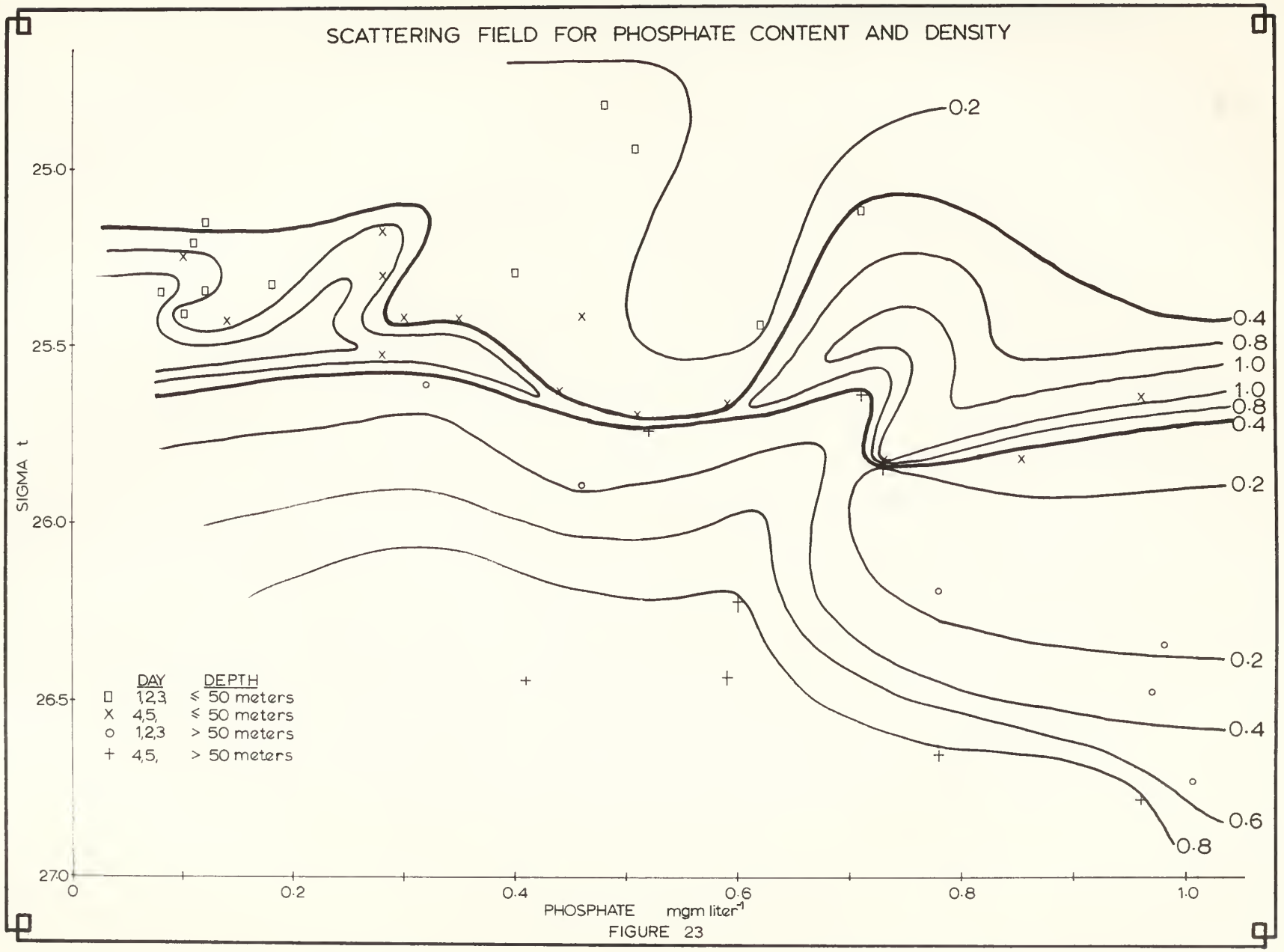
SCATTERING FIELD FOR PHOSPHATE CONTENT AND DENSITY
SIGMA t
25·0
25·5
26·0
26·5
27·0
0
0·2
0·4
0·6
0·8
1·0
PHOSPHATE mgm liter⁻¹
DAY DEPTH
1,2,3 ≤ 50 meters
4,5, ≤ 50 meters
1,2,3 > 50 meters
4,5, > 50 meters
0·2
0·4
0·8
1·0
1·0
0·8
0·4
0·2
0·2
0·4
0·6
0·8

FIGURE 23

Thesis
B24255 Bassett
79478
An investigation of the vertical variation of light scattering in Monterey Bay, Calif.

Thesis
B24255 Bassett
79478
An investigation of the vertical variation of light scattering in Monterey Bay, Calif.